

INVESTIGATING THE ROLE OF SIRT1 EXON 2 IN LIVER PHYSIOLOGY

Dissertation Submitted to Bharathidasan University
in partial fulfillment of the requirement for the Degree of

Master of Science in Life Sciences

Submitted by

Mr. U. HEARTWIN RAJ

Reg. No. LS19012

Under the guidance of

PROF. ULLAS KOLTHUR SEETHARAM, PhD, FASc, FNASc, FNA

DEPARTMENT OF BIOLOGICAL SCIENCES,

TATA INSTITUTE OF FUNDAMENTAL RESEARCH, MUMBAI



SCHOOL OF LIFE SCIENCES

BHARATHIDASAN UNIVERSITY

(Accredited with A+ Grade by NAAC in the Third Cycle)

TIRUCHIRAPPALLI - 620 024

TAMIL NADU, INDIA

JUNE 2024



Tata Institute of Fundamental Research

Homi Bhaha Road, Colaba, Mumbai

CERTIFICATE

I certify that the research work presented in this thesis titled “**Investigating the role of SIRT1 exon 2 in Liver physiology**” has been carried out by **Mr. U. Heartwin Raj** Reg. No. **LS19012** under my supervision and this is his bonafide work. The research work is original and has not been submitted for any other degree of this or any other University. Further, he was a regular student and has worked under my guidance as a full-time student at Tata Institute of Fundamental Research, Colaba, Mumbai until the submission of the thesis to the Bharathidasan University, Tiruchirappalli, Tamil Nadu.

Date: 31-05-2024

Place: Mumbai

A handwritten signature in purple ink, appearing to read 'S. Srinivas', is written over a horizontal line.

Signature with designation

Dr. V. Ravikumar, Ph.D.
Professor

Phone :91-431-2407071 Ext 485
Mobile :91- 9444162763
Email :ravikumarbdu@gmail.com
drvrr@bdu.ac.in



BHARATHIDASAN UNIVERSITY
Accredited with A+ Grade by NAAC
in the Third Cycle
DEPARTMENT OF BIOCHEMISTRY
(DST-FIST Sponsored)
Tiruchirappalli, Tamil Nadu – 620 024
Phone :91-431-2407071
Fax :91-431-2407045

12-6-2024

CERTIFICATE

This is to certify that this dissertation entitled **“Investigating the Role of SIRT1 Exon 2 in Liver Physiology”** submitted to Bharathidasan University, Tiruchirappalli 620 024, for the award of Degree of Master of Science in Life Science is an authentic record of original work carried out by **Heartwin Raj. U, Reg. No: LS19012**, under my supervision as Internal Guide at Tata Institute of Fundamental Research, Mumbai. I further certify that no part of this dissertation has previously formed the basis for the award for the Candidate of any Degree, Diploma, Associateship, Fellowship or similar title of this or any other University or Society.

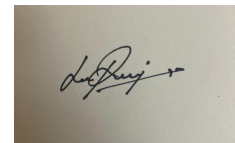
Dr. V. RAVIKUMAR

DECLARATION

This is to state that the work embodied in this thesis titled **“Investigating the role of SIRT1 Exon 2 in liver physiology”** forms my own contribution to the research work carried out under the guidance of Prof. Ullas Kolthur-Seetharam at Department of Biological Sciences, Tata Institute of Fundamental Research, Colaba, Mumbai. This work has not been submitted of any degree of this university or any other University. Whenever references have been made to previous work of others, it has been clearly indicated as such included in the Bibliography.

Place: Tiruchirappalli

Date: 12-06-2024

A rectangular box containing a handwritten signature in black ink. The signature is cursive and appears to read 'L. R. Singh'.

Signature of the Candidate

ACKNOWLEDGEMENTS

The journey of writing this dissertation is my first encounter with scientific research. While I have strived to do my best, I am humbled and grateful for the invaluable contributions of several individuals who have played a significant role in its completion.

First and foremost, I would like to express my deepest gratitude to ***Prof. Ullas Kolthur-Seetharam***, Professor in the Department of Biological Sciences at the Tata Institute of Fundamental Research. I am immensely grateful to him for giving me this opportunity and allowing me to work in his lab. His unwavering supports, inspiration, and guidance have been instrumental throughout this journey. I would also like to thank him for providing the necessary resources and creating an environment conducive to learning and growth.

I want to express my sincere gratitude to ***Arushi S*** for her never-ending cooperation during the entire coursework of this thesis. Without her guidance and persistent help, this dissertation would not have been possible. She has been an extremely patient and helpful mentor. Her friendly and down-to-earth approach always instilled confidence in me. Her guidance, support and encouragement made me learn the finer details of my work. I am indebted for her critical inputs, ideas, and guidance throughout the completion of the project.

I would also like to express my gratitude to my fellow lab members, ***Sandra, Subhash, Arshdeep, Souparno and Shreyam***, for their unwavering encouragement and assistance during times of need. Their support and camaraderie have made this journey more fulfilling and enjoyable.

My deepest gratitude goes to my ***dear parents and family*** for their unwavering belief in me and my endeavors. Their constant support and unwavering faith have been a driving force throughout this journey.

Lastly, I would like to thank all those who have directly or indirectly contributed to the successful completion of this dissertation. Your support, encouragement, and belief in me have been truly invaluable.

Heartwin Raj

Table of Contents	
LIST OF FIGURES	V
LIST OF TABLES	VI
LIST OF ABBREVIATIONS	VII
CHAPTER 1	1
1. Introduction	2
1.1. Energy Metabolism in the Liver	2
1.1.1. Carbohydrate metabolism	2
1.1.1.1. Glycogenesis	2
1.1.1.2. Glycogenolysis	2
1.1.1.3. Gluconeogenesis	3
1.1.1.4. Glycolysis	3
1.1.2. Lipid metabolism	4
1.1.2.1. Lipogenesis	4
1.1.2.2. Fatty acid oxidation	4
1.1.2.3. Lipoprotein synthesis	4
1.1.2.4. Phospholipid and cholesterol synthesis	4
1.2. Effects of fasting and feeding mechanisms in liver metabolism	5
1.3. Sirtuins	6
1.3.1. SIRT1	7
1.3.2. SIRT1 on liver metabolism	7
1.4. SIRT1-ΔE2	8
CHAPTER 2	9
2. Literature Review	10
2.1. SIRT1 – NAD ⁺ dependent deacetylase	10
2.2. SIRT1 – Master metabolic regulator	10
2.2.1. Hepatic glucose and lipid metabolism	11
2.2.2. Important modulator of maturation of adipose tissues	12
2.2.3. Regulation of pancreatic insulin secretion	12
2.2.4. Central control of metabolic homeostasis	13
2.2.5. Key transcriptional regulator of inflammation	13
2.2.6. Regulation of circadian rhythm	14

2.3. Impact of fasting and feeding on liver metabolism	14
2.4. Hepatic transcriptional responses to fasting and feeding	15
2.4.1. Lipid metabolism	15
2.4.1.1. Regulation of fatty acid synthesis and ketogenesis	15
2.4.1.2. Regulation of lipogenesis and cholesterol synthesis	16
2.4.2. Glucose metabolism	19
2.4.2.1. Regulation of glucose metabolism during fasting	19
2.4.2.2. Regulation of glucose metabolism during feeding	20
2.5. SIRT1 in lipid and glucose metabolism	21
2.5.1. Lipid metabolism	22
2.5.2. Glucose metabolism	23
2.6. Hepatocyte specific deletion of SIRT1	24
CHAPTER 3	26
3. Materials and Methods	27
3.1. Materials	27
3.1.1. Chemical reagents	27
3.1.2. DNA molecular size marker	29
3.1.3. Prestained protein ladder	29
3.2. Methods	29
3.2.1. Generation of liver specific SIRT1- Δ E2 mouse models (EC17IC)	29
3.2.2. Tail clip digestion	31
3.2.3. Designing of primers	31
3.2.4. Genotyping by PCR	32
3.2.5. Preparation of Lysate	34
3.2.6. BCA assay	35
3.2.7. Western blot analysis	35
3.2.7.1. SDS-PAGE	35
3.2.7.2. Membrane transfer	37
3.2.7.3. Blocking	37
3.2.7.4. Antibody incubations	38
3.2.7.5. Chemiluminescent detection	38
3.2.8. Isolation of RNA by TRIzol	38
3.2.9. Synthesis of cDNA	39

3.2.10. Quantitative PCR	40
3.2.11. PCR for E2 knockout confirmation in mRNA level	41
3.2.12. Intraperitoneal Glucose Tolerance Test	44
CHAPTER 4	45
4. Results	46
4.1. Genotyping by PCR	46
4.2. Lysate preparation and BCA assay	49
4.3. Western blot analysis to confirm SIRT1-ΔE2 knockout	49
4.4. Isolation RNA	50
4.5. Quantitative-PCR	51
4.6. Confirmation of SIRT1-ΔE2 knockout in cDNA	52
4.7. Western blot for gene expression analysis in 24 months old mice liver samples	54
4.8. Intraperitoneal Glucose Tolerance Test	57
CHAPTER 5	59
5. Discussion	60
5.1. Future perspectives	62
CHAPTER 6	64
6. Summary and Conclusion	65
CHAPTER 7	67
7. References	68
CHAPTER 8	78
8. Appendix	79
8.1. Preparation of Agarose gel	79
8.2. RNA concentration measurement	79

LIST OF FIGURES

Figure 1.1: Overview of Carbohydrate metabolism	3
Figure 1.2: Metabolic map of Lipids	5
Figure 1.3: Feeding and fasting mechanisms in liver metabolism	6
Figure 1.4: SIRT1 is an NAD ⁺ dependent protein deacetylase	8
Figure 2.1: SIRT1 is a master metabolic regulator in different metabolic tissues	11
Figure 2.2: Regulation of fatty acid oxidation and ketogenesis	16
Figure 2.3: Regulation of lipogenesis and cholesterol synthesis	18
Figure 2.4: Regulation of gluconeogenesis and glycogenolysis	20
Figure 2.5: Regulation of glycolysis and glycogen synthesis	21
Figure 2.6: Transcriptional regulation of lipid metabolism related genes by SIRT1 in liver	23
Figure 2.7: Transcriptional regulation of glucose metabolism related genes by SIRT1 in liver	24
Figure 3.1: Schematic representation of generation of liver specific SIRT1-ΔE2 mice	30
Figure 3.2: Schematic representation of Albumin-Cre genotyping PCR parameters employed during execution	34
Figure 3.3: Schematic representation of E2lox/lox genotyping PCR parameters employed during execution	34
Figure 3.4: Schematic representation of PCR parameters employed during execution	43
Figure 4.1: Genotyping and visualization of EC17IC A&B Albumin-Cre and E2lox/lox	46
Figure 4.2: Standard curve for BCA protein assay of liver and testes	49
Figure 4.3: SIRT1-ΔE2 knockout confirmation on western blots	50
Figure 4.4: Isolation and visualization of RNA	51
Figure 4.5A: Melt curve for Actin in cDNA	52
Figure 4.5B: qPCR amplification of Actin in cDNA	52
Figure 4.6: Confirmation of SIRT1-ΔE2 knockout in cDNA	53
Figure 4.7A: Quantified protein levels	55
Figure 4.7B: Fold change levels	56
Figure 4.8: Blood glucose levels over time	58

LIST OF TABLES

Table 1.1: SIRT1 regulates cell metabolism by interacting with certain factors	7
Table 3.1: Reagents used for genotyping	27
Table 3.2: Reagents used for lysate preparation	27
Table 3.3: Reagents used for BCA assay	27
Table 3.4: Reagents used for SDS-PAGE	27
Table 3.5: Reagents used for western blot	28
Table 3.6: Antibodies used for western blot	28
Table 3.7: Reagents used for isolation of RNA	28
Table 3.8: Reagents used for cDNA	29
Table 3.9: Reagents used for qPCR	29
Table 3.10: Reaction mixture for tail clip digestion	31
Table 3.11: Primers used for genotyping	31
Table 3.12: Primers used for qPCR	31
Table 3.13: Primers used for E2 knockout confirmation	32
Table 3.14: Reaction mixture for Albumin-Cre genotyping PCR	32
Table 3.15: Thermal cycles for Albumin-Cre genotyping PCR amplification	33
Table 3.16: Reaction mixture for E2lox/lox genotyping PCR	33
Table 3.17: Thermal cycles for E2lox/lox genotyping PCR amplification	33
Table 3.18: Aliquot volumes for RIPA buffer with the inhibitors	35
Table 3.19: Components for 6% Resolving gel	36
Table 3.20: Components for Stacking gel	36
Table 3.21: Composition of Transfer buffer	37
Table 3.22: Composition of 1x TBST	38
Table 3.23: Composition of 70% EtOH	39
Table 3.24: Reaction mixture A for cDNA synthesis	40
Table 3.25: Reaction mixture B for cDNA synthesis	40
Table 3.26: Reaction mixture for Actin qPCR	41
Table 3.27: Thermal cycles for qPCR amplification	41
Table 3.28: Reaction mixture of PCR for SIRT1 full length	42
Table 3.29: Reaction mixture of PCR for SIRT1-ΔE2	42
Table 4.1: IP-GTT Data	57

LIST OF ABBREVIATIONS

ATP: Adenosine triphosphate

ADP: Adenosine diphosphate

LDL: Low Density Lipoprotein

VLDL: Very Low-Density Lipoprotein

HDL: High Density Lipoprotein

NAD⁺: Nicotinamide adenine dinucleotide

NADH: Nicotinamide adenine dinucleotide+ hydrogen

CREB: Cyclic AMP-response element binding protein

CRTC2: CREB-regulated Transcription Coactivator 2

FOXO1: Forkhead box protein O1

PGC-1 α : Peroxisome proliferator-activated receptor-gamma coactivator

HIF1 α : Hypoxia-inducible factor 1-alpha

PGAM-1: Phosphoglycerate mutase

SREBP: Sterol Regulatory Element-binding Protein

AMPK: AMP activated protein kinase

PPAR- γ : Peroxisome proliferator-activated receptor gamma

Nampt: Nicotinamide phosphoribosyltransferase

POMC: Pro-opiomelanocortin

AgRP: Agouti-Related Protein

ChREBP: Carbohydrate response element-binding protein

HDAC: Histone deacetylase

FXR: Farnesoid X receptor

LXR: Liver X receptor

PKA: Protein kinase A

LKO: Liver Knockout

KO: Knockout

WT: Wildtype

PCR: Polymerase Chain Reaction

NCBI: National Center for Biotechnology Information

BLAST: Basic Local Alignment Search Tool

MCT: Micro centrifuge tube

WAT: White Adipose Tissue

BAT: Black Adipose Tissue

LCFA: Long Chain Fatty Acid

FGF21: Fibroblast Growth Factor 21

GR: Glucocorticoid Receptor

G6Pase: Glucose 6 phosphatase

PEPCK: Phosphoenolpyruvate Carboxykinase

Bsep: Bile salt export pump

Mcadh: Medium chain acyl-CoA dehydrogenase

BCA: Bicinchoninic Acid

kb: Kilo bytes

bp: Base pairs

kDa: Kilo Dalton

Alb: Albumin

CHAPTER 1

INTRODUCTION

1. Introduction

1.1 Energy Metabolism in the Liver

The liver is a key metabolic organ which governs body energy metabolism. It acts as a hub to metabolically connect to various tissues, including skeletal muscle and adipose tissue. Food is digested in the gastrointestinal tract, and glucose, fatty acids, and amino acids are absorbed in the bloodstream and transported to the liver through the portal vein circulation system (Liangyou Rui, 2014). Liver functions as a master regulator of metabolic homeostasis, exerting crucial control over lipid and glucose balance, thereby ensuring efficient energy utilization within the body. Among the important functions performed by the liver is maintaining of blood glucose levels during fasting by releasing glucose from glycogen and synthesis of glucose from amino acids, fats and lipids (Alamri, Z. Z, 2018). In the fed state, glycolytic products are used to synthesize fatty acids through *de novo* lipogenesis. Long-chain fatty acids are incorporated into triacylglycerol, phospholipids, and cholesterol esters in hepatocytes, and these complex lipids are stored in lipid droplets and membrane structures, or secreted into the circulation as VLDL particles (Liangyou Rui, 2014). The major metabolic functions of the liver can be broadly discussed in two main categories.

1.1.1 Carbohydrate Metabolism

The liver plays a unique role in controlling carbohydrate metabolism by maintaining glucose concentrations in a normal range. This is achieved through several processes regulating either glucose breakdown or synthesis in hepatocytes (Raddatz, D., & Ramadori, G, 2007) (**Figure 1.1**).

1.1.1.1 Glycogenesis

This is the process by which the liver converts excess glucose (entering the circulation after a meal following digestion of complex carbohydrates) into glycogen, the stored form of carbohydrate in the liver. This process is stimulated by insulin released from the pancreas during the fed state (Mitra, V., & Metcalf, J., 2009).

1.1.1.2 Glycogenolysis

The liver is also involved in the breakdown of glycogen into glucose molecules that can be transported to other tissues for generating energy in the form of ATP in response to low circulating levels of glucose in the fasting state (Mitra, V., & Metcalf, J., 2009).

1.1.1.3 Gluconeogenesis

This is the process by which the liver synthesizes glucose from amino acids and other non-hexose carbohydrates. This process takes place particularly when the hepatic glycogen are depleted (Mitra, V., & Metcalf, J., 2009).

1.1.1.4 Glycolysis

Glycolysis is a series of reactions that extract energy from glucose by spitting it into two three-carbon molecules called pyruvates. It occurs in both aerobic and anaerobic states. In aerobic conditions, pyruvate enters the citric acid cycle and undergoes oxidative phosphorylation leading to the net production of 32 ATP molecules. In anaerobic conditions, pyruvate converts to lactate which results in the production of 2 ATP molecules (Chaudhry, R & Varacallo, M, 2018).

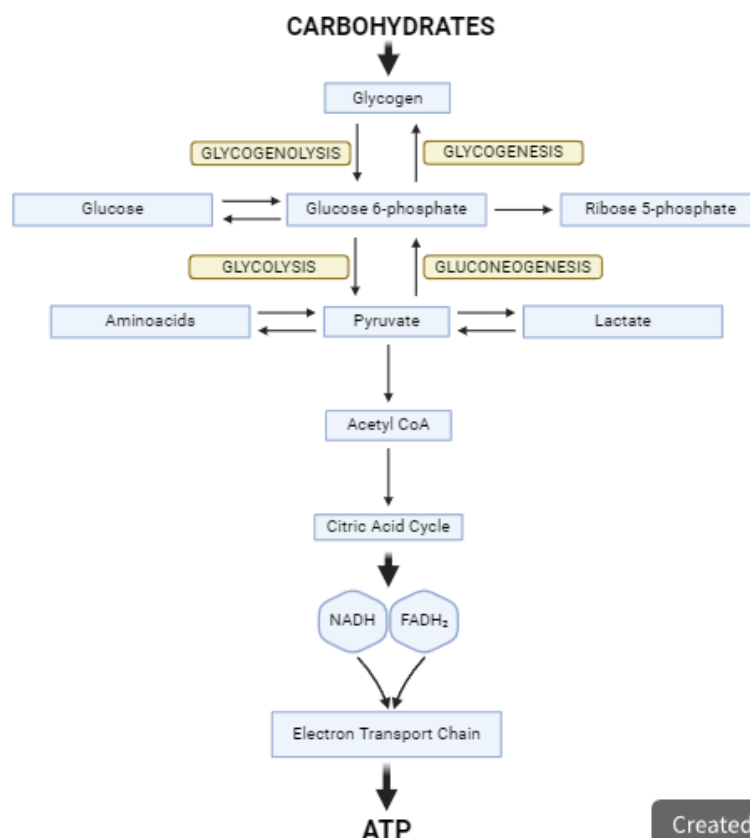


Figure 1.1: Overview of Carbohydrate Metabolism

Carbohydrate metabolism occurs through the processes of converting glucose into glycogen (Glycogenesis), breaking down of glucose into pyruvate (Glycolysis) and synthesis of glucose from glycogen (Glycogenolysis) and from pyruvate (Gluconeogenesis). (Created with BioRender.com)

1.1.2 Lipid Metabolism

The liver plays a key role in lipid metabolism, which is the hub of fatty acid synthesis and lipid circulation through lipoprotein synthesis (Nguyen et al., 2008).

1.1.2.1 Lipogenesis

This is the process by which fatty acids are synthesized from acetyl CoA molecules derived from the catabolism of carbohydrates in the fed state (Mitra, V., & Metcalf, J., 2009).

1.1.2.2 Fatty acid oxidation

Initially triglycerides are hydrolysed into glycerol and fatty acids. The fatty acids are oxidized into acetyl CoA, which enters the citric acid cycle, producing ATP, CO₂ and water. The glycerol molecules are converted into dihydroxyacetone molecules, which may either be converted into pyruvic acid or undergo gluconeogenesis (Mitra, V., & Metcalf, J., 2009).

1.1.2.3 Lipoprotein synthesis

In addition, the liver synthesizes lipoproteins such as LDL, VLDL and HDL. These transport fatty acids, phospholipids and cholesterol in the circulation to various tissues in the body (Mitra, V., & Metcalf, J., 2009).

1.1.2.4 Phospholipid and cholesterol synthesis

The liver also synthesizes phospholipids and cholesterol in the body, some of which are bound to lipoproteins and are available to other tissues of the body while the rest are excreted through bile as cholesterol or converted into bile acids (Mitra, V., & Metcalf, J., 2009).

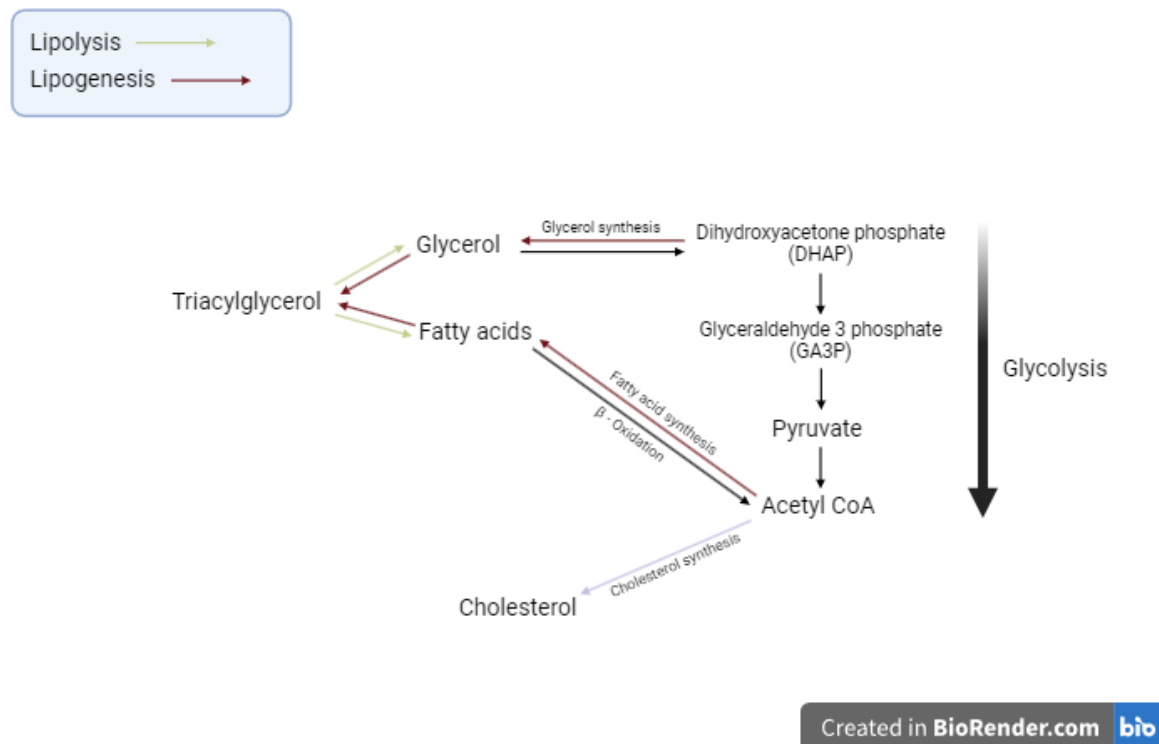


Figure 1.2: Metabolic map of Lipids

The process by which the triacylglycerol breaks down into glycerol and fatty acids are known as Lipolysis and the process by which the fatty acids and glycerol is synthesized for the production of triacylglycerol is Lipogenesis. (Created with BioRender.com)

1.2 Effects of fasting and feeding mechanisms in liver metabolism

Mammals undergo regular cycles of fasting and feeding that engage dynamic transcriptional responses in metabolic tissues. The liver is a central hub for coordination of fasting-feeding transitions given its role in maintaining blood glucose levels, processing dietary nutrients and regulating whole body energy metabolism. During fasting the liver is the target of hormones such as glucagon, which shift it into an energy production mode. In the postprandial state, signalled by insulin and the influx of dietary carbohydrates, liver suppresses the production of glucose and switches to using it for replenishing the used-up glycogen stores (Bideyan L et al., 2021) (**Figure 1.3**).

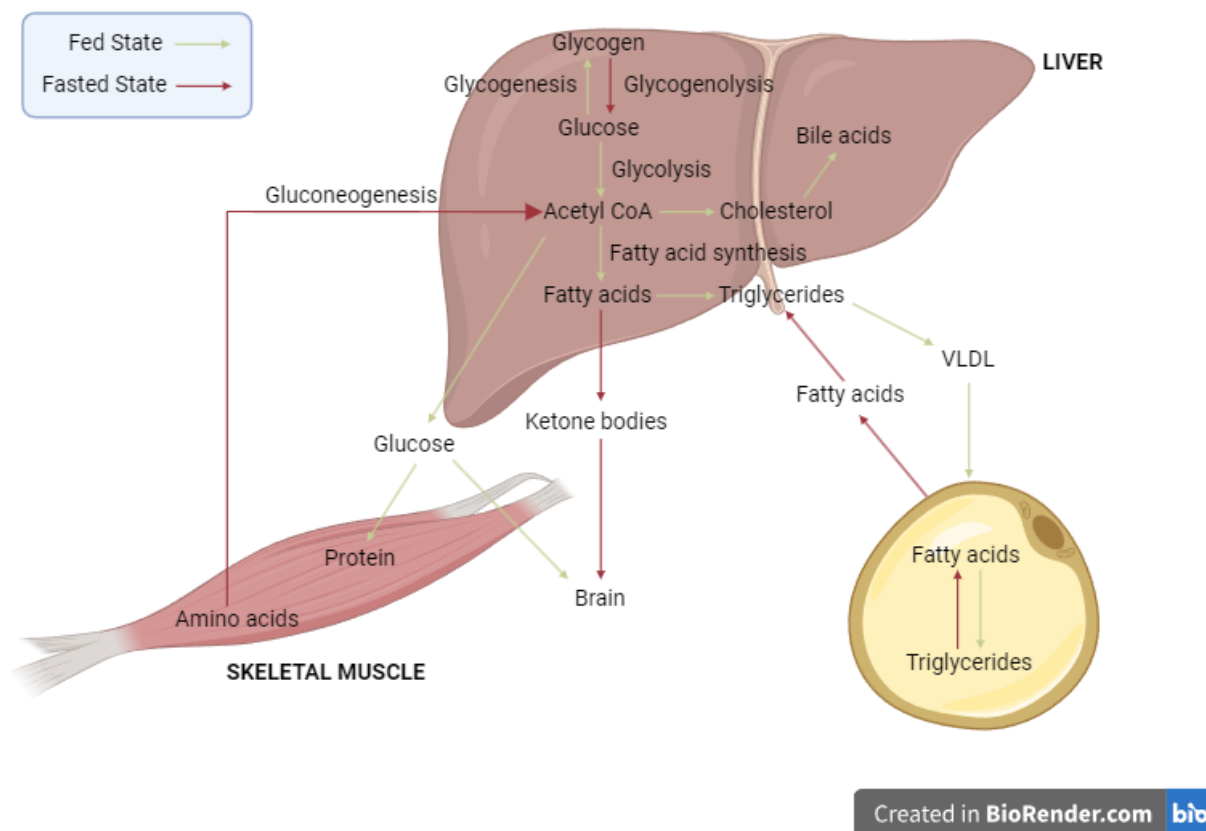


Figure 1.3: Feeding and fasting mechanisms in liver metabolism

During the fed state, glucose is stored in the liver as glycogen. Glucose goes through glycolysis to generate acetyl-CoA, which is used to synthesize fatty acids or cholesterol. Cholesterol is catabolized to bile acids. Fatty acids are esterified to glycerol to form triglycerides, which are assembled to VLDL for secretion and transport to adipocytes for storage and other tissues for energy production. Glucose is up taken by muscle and other tissues for energy production. In the fasted state, triglycerides in adipocytes are hydrolysed to free fatty acids, which are transported to the liver for synthesis of triglycerides and ketone bodies. Ketone bodies are utilized for energy production in the brain and muscle. Under long term starvation, muscle proteins are degraded to amino acids, which are transported to the liver for synthesis of glucose by gluconeogenesis (Created with BioRender.com) (Adapted from Chiang, J., 2014).

1.3 Sirtuins

Sirtuins, a family of highly conserved protein modifying enzymes founded by the yeast silent information regulator 2 (Sir2) protein, are NAD^+ -dependent protein deacetylases and/or ADP-ribosyltransferases (Li X., 2013). Humans have seven sirtuins (SIRT1 – SIRT7), which differ in their subcellular localization. SIRT1, SIRT6 and SIRT7 are nuclear sirtuins, which regulate several critical transcription factors of many metabolic pathways. SIRT2 is located primarily in cytoplasm and is able to regulate cellular mitosis to prevent genomic instability. SIRT3,

SIRT4 and SIRT5 are located in mitochondria. SIRT3 has been demonstrated to be a legitimate tumor suppressor by regulating mitochondrial energy homeostasis, suppressing ROS production, whereas SIRT4 functions as a tumor suppressor as well by mediating a DNA damage dependent block in glutamine metabolism (Zhu, Y et al., 2013).

1.3.1 SIRT1

Among the seven sirtuins that the mammalian genome encodes, SIRT1 is the ortholog of the yeast Sir2 protein and a nuclear NAD⁺ dependant protein deacetylase (**Figure 1.4**). This sirtuin is a nuclear metabolic sensor that directly couples the cellular metabolic status to the chromatin structure and the regulation of gene expression through deacetylation of histones, transcription factors and transcription co-factors. Since it plays a vital role in metabolism, development, reproduction, it is not surprising that SIRT1 affects more complex biological phenomena such as aging and disease. Therefore, understanding the role of SIRT1 in energy metabolism will likely provide insights into therapeutic strategies designed towards metabolic diseases and possibly aging (Li X., 2013).

1.3.2 SIRT1 on liver metabolism

Through its ability to deacetylate target protein, SIRT1 influences cell metabolism by a variety of means, especially in glucose and lipid metabolism (**Table 1.1**) (Ye, X et al., 2017).

Table 1.1: SIRT1 regulates cell metabolism by interacting with certain factors

Interacting Factor with SIRT1	Effects
CRTC2	Gluconeogenesis ↓
FoxO1	Gluconeogenesis ↑
PGC-1 α	Glycolysis ↓; Gluconeogenesis ↑
HIF1 α	Glycolysis ↓
PGAM-1	Glycolysis ↓
SREBP	Lipid synthesis ↓; fat storage ↓
AMPK	Fatty acid synthesis ↓
PPAR- γ	Fatty acid accumulation ↓; fat storage ↓

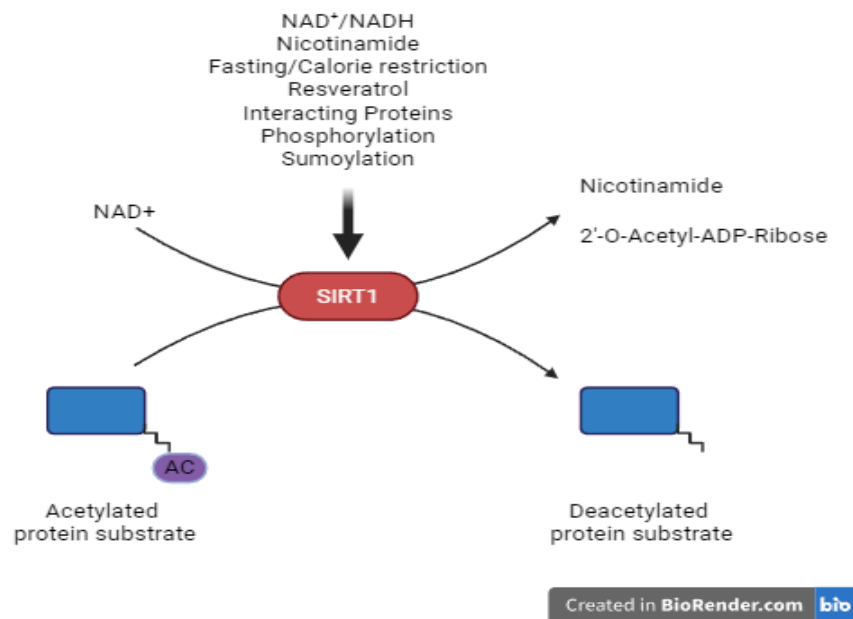


Figure 1.4: SIRT1 is an NAD⁺-dependent protein deacetylase

SIRT1 splits NAD⁺ into nicotinamide and ADP-ribose, then transfers the acetyl group from the protein substrate to the 2'-OH group of ribose ring in the ADP-ribose molecule. Nutritional, hormonal and environmental signals can modulate the deacetylase activity of SIRT1 through changes of the cellular NAD⁺ levels, alterations in the expression of SIRT1 protein, or posttranslational modifications/interactions on SIRT1 protein. (Created with BioRender.Com) (Adapted from Li X., 2013)

1.4 SIRT1-ΔE2

Gain-/loss-of-function studies in mice have established that SIRT1 alterations affect physiology and either protect or predispose the organism to various pathophysiological conditions. It is important to investigate the molecular mechanisms that control SIRT1 activity and specificity under physiological conditions in a tissue specific manner. (Deota. S., et al., 2017). So, it is necessary to understand the intrinsic catalytic activity of SIRT1 in the absence of exon 2 specifically in liver, which can determine the substrate interactions and downstream functions of SIRT1 in cellular metabolism and aging.

CHAPTER 2

LITERATURE REVIEW

2. Literature Review

2.1 SIRT1 – NAD⁺ dependent deacetylase

SIRT1 functions as a highly versatile protein deacetylase, targeting a vast array of protein substrates (Haigis, M. C., 2010). However, the activity of SIRT1 is tightly controlled by the cellular levels of NAD⁺ (**Figure 1.4**). NAD⁺ is an essential coenzyme found in all living cells and can be viewed in four main categories, 1. De Novo Synthesis, 2. Scavenging Pathways from preformed precursors (nicotinic acid, nicotinamide riboside and nicotinic acid riboside), 3. Core Recycling Pathway through nicotinamide. Finally, 4. ADPR-transfer/NAD hydrolysis, which occurs through a variety of enzymatic pathways, leading to cleavage of the N-glycosidic bond of nicotinamide to the ribose ring, thereby liberating nicotinamide and providing an ADPR-nucleophile product. Thus, three general types of synthesis pathways converge to produce NAD⁺ while consumption pathways comprised of several types of NAD⁺ consumers deplete NAD⁺ (Yang, Y., & Sauve, A., 2016). NAD⁺ is involved in redox reactions through electron transfer, in which it can readily switch from oxidizing NAD⁺ to reducing NADH, and vice versa (Houtkooper, R. H et al., 2010). Therefore, NAD⁺ and NADH are extensively utilized in an array of metabolic reactions, and the cellular level of NAD⁺ is an important factor of the cellular energy status. As a result, SIRT1 provides a molecular link between the cellular energy status and the adaptive transcriptional responses (Bordone. L et al., 2005).

Not surprisingly, the activity of SIRT1 is closely controlled by different environmental cues that can change the cellular NAD⁺ availability. For instance, a low-energy status that increases cellular levels of NAD⁺, such as fasting, caloric restriction (CR) and exercise has been shown to stimulate SIRT1 activity (JT, R et al., 2005). On the other hand, a high-energy status that decreases cellular NAD⁺ levels, including high-fat diet feeding and acute inflammatory responses, reduces SIRT1 activity (Yoshino, J et al., 2011). In addition, direct manipulation of the biosynthesis and catabolism of NAD⁺ can also alter cellular NAD⁺ levels and thereby SIRT1 activity. For example, increasing the activity of Nampt, the rate-limiting enzyme in the salvage pathway of NAD⁺ biosynthesis, enhances the levels of NAD⁺ and activity of SIRT1 (Skokowa J et al., 2009). Whereas decreasing the activity of Nampt leads to reduced NAD⁺ levels and SIRT1 activity (Van der Veer et al., 2007).

2.2 SIRT1 – Master Metabolic regulator

SIRT1 acts as a central regulator of systemic metabolic homeostasis through its deacetylation of a diverse array of transcription factors and co-factors (**Figure 2.1**).

2.2.1 Hepatic Glucose and Lipid Metabolism

The liver is a central metabolic organ that controls several key aspects of lipid and glucose metabolism in response to nutritional and hormonal signals (Van den Berghe, G, 1991). SIRT1 is a key modulator of gluconeogenesis in response to fasting. It has been shown that during the early stages of long-term fasting, SIRT1 inhibits CRTC2, a coactivator of CREB that is important for cAMP/CREB mediated activation of gluconeogenesis genes, leading to reduced gluconeogenesis (Liu Y et al., 2008). Yet the prolonged fasting increases SIRT1 mediated deacetylation and activation of FOXO1 and PGC-1 α , an essential coactivator for number of transcription factors, resulting in increased fatty acid oxidation and improved glucose homeostasis (JT, R et al., 2005). These complex interactions between key modulators like SIRT1 and multiple transcription factors results in a well-orchestrated fasting response.

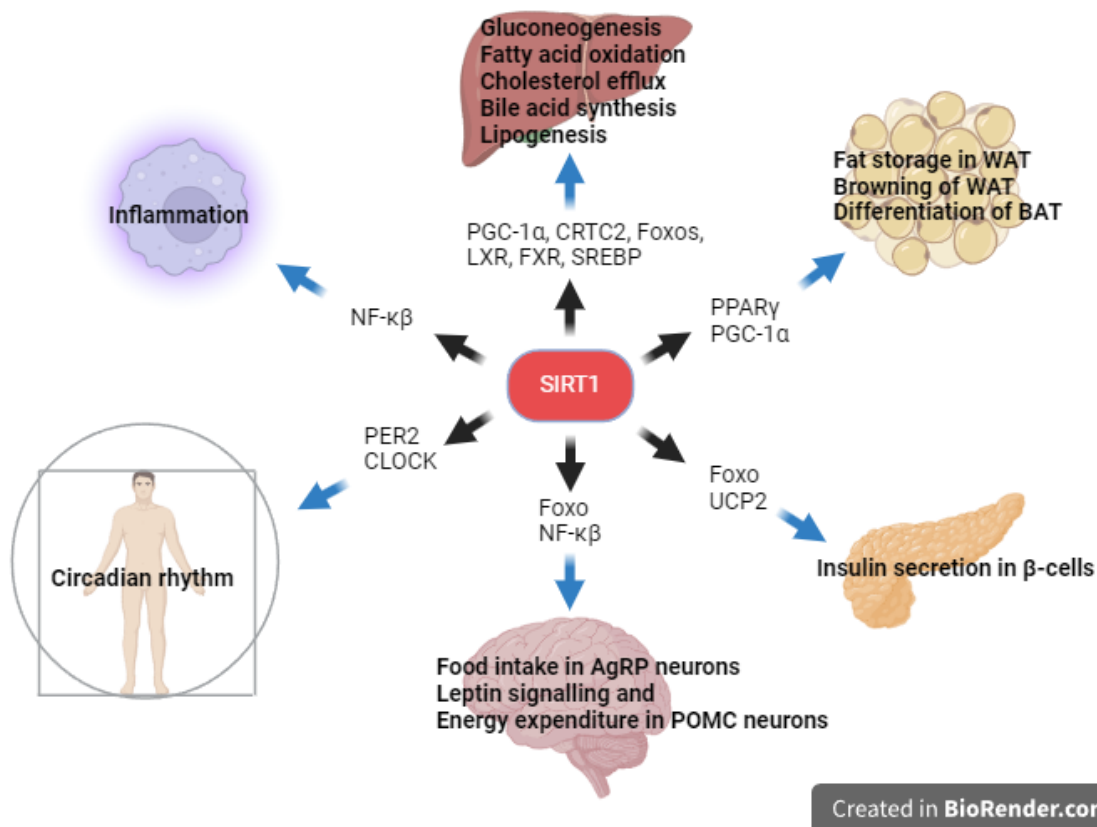


Figure 2.1: SIRT1 is a master metabolic regulator in different metabolic tissues

SIRT1 couples the deacetylation of a number of transcription factors and co-factors to the cleavage of NAD⁺, an indicator of cellular metabolic status, playing a vital role in metabolism, inflammation, development and reproduction, which will ultimately affect the process of aging and disease. (Created with BioRender.com) (Adapted from Li X, 2013)

Hepatic SIRT1 also plays an important role in hepatic fatty acid metabolism. It has been shown via adenoviral knockdown of SIRT1 that reduced levels of SIRT1 results in reduced expression

of fatty acid β -oxidation genes in the liver of fasted mice (Rodgers, J.T et al., 2007). Purushotham A et al in 2009 showed that specific deletion of the exon 4 of the mouse hepatic SIRT1 gene which results in a truncated inactive SIRT1 protein, impairs fatty acid β -oxidation through the PPAR α /PGC-1 α pathway, thereby increasing the susceptibility of mice to high-fat-diet-induced dyslipidemia, hepatic steatosis, inflammation and endoplasmic reticulum stress. Consistently, a complete deletion of hepatic SIRT1 leads to the development of liver steatosis even under normal feeding conditions (wang, R. H., et al 2010). Conversely, hepatic overexpression of SIRT1 mediated by adenovirus attenuates hepatic steatosis and ER stress and restores glucose homeostasis in mice (Li Y et al., 2011), confirming the essential role of SIRT1 in maintaining hepatic glucose and lipid homeostasis.

2.2.2 Important modulator of Maturation of Adipose tissues

Adipose tissues, including white adipose tissue (WAT) and brown adipose tissue (BAT), are important metabolic tissues involved in fat storage, body insulation and body temperature regulation. Adipose tissues originate from the differentiation of lipoblasts, and one of the primary factors involved in adipose tissue differentiation is the nuclear receptor PPAR γ (Tontonoz, P et al., 2008). SIRT1 has been shown to repress PPAR γ in WAT, thereby suppressing the expression of adipose tissue markers, such as the mouse adipocyte Protein 2 gene (Picard et al., 2004). Consistently, genetic ablation of SIRT1 in adipose tissue leads to increased adiposity and insulin resistance (Chalkiadaki, A & Guarente, L, 2012). The treatment of mice on a high-fat diet with resveratrol, a polyphenol that activates SIRT1 in cells directly or indirectly has also been shown to protect against high-fat-induced obesity and metabolic derangements (Baur, J. A et al., 2006). These findings suggest a cooperative role for SIRT1 with lipid sensing transcription factors, such as PPAR γ , in dynamically regulating WAT gene expression in response to fluctuations in systemic nutrient availability.

2.2.3 Regulation of Pancreatic insulin secretion

Pancreatic β cells are specialized endocrine cells located in the islets of Langerhans in pancreas. They are systemic metabolic sensors that synthesize and store insulin and release insulin in response to the increase in blood glucose levels. SIRT1 has been shown to be a positive regulator for pancreatic insulin secretion, which in turn triggers glucose uptake and utilization. It has been shown that, increased dosage of SIRT1 specifically in Pancreatic β cells improves glucose tolerance and enhances insulin secretion in response to glucose in mice (Moynihan, K. A et al., 2005). Whereas systemic deletion of SIRT1 impairs glucose stimulated insulin secretion (Bordone, L et al., 2006). In both studies, SIRT1 has been shown to promote insulin

secretion through transcriptional repression of uncoupling protein 2 (UCP2). Collectively, these observations indicate that SIRT1 is a vital regulator of pancreatic insulin secretion in response to the nutrient availability.

2.2.4 Central control of metabolic homeostasis

The brain plays a critical role in the regulation of systemic energy homeostasis. Through assessment and integration of peripheral metabolic, endocrine and neuronal signals, central nervous circuits are able to orchestrate a modulating program on both behavioural patterns and peripheral metabolism to adapt acute and chronic energy requirements (Horvath, T. L et al., 2004). In the hypothalamus, the anorexigenic POMC expressing neurons and the orexigenic agouti-related protein (AgRP) expressing neurons are the major regulators of feeding and energy expenditure (Morton, G. J et al., 2006). The POMC neurons produce satiety peptides thereby inhibiting food intake after feeding, while the AgRP neurons promote feeding in response to fasting and CR. It appears that SIRT1 displays distinct functions in these two neuron populations. Hypothalamic SIRT1 activity increases acetylation of FOXO1, resulting in increased POMC and decreased AgRP expressions, thereby decreasing food intake and body weight gain (Cakir, I et al., 2009). On the contrary, specific deletion of SIRT1 in POMC neurons in mice causes a blunted response to leptin signalling and reduced energy expenditure, leading to hypersensitivity to diet-induced obesity (Ramadori, G et al., 2010). In summary, SIRT1 activity appears to be an important player in the central regulation of nutrient sensing.

2.2.5 Key transcriptional regulator of inflammation

Macrophage activation and infiltration into resident tissues is known to mediate local inflammation and is a hallmark of metabolic syndrome (Odegaard, J. I et al., 2007). This infiltration-induced local inflammation has been increasingly recognized as a causal factor leading to the development of the cluster of diseases surrounding metabolic syndrome (Suganami, T., & Ogawa, Y, 2010). In mice, modest overexpression of SIRT1 leads to suppression of the inflammatory response, whereas whole-body insufficiency of SIRT1 induces systemic inflammation upon high-fat diet challenge (Pfluger, P. T et al., 2008). Furthermore, deletion of SIRT1 in hepatocytes results in increased local inflammation under high fat diet (Purushotham A et al., 2009). It has been shown that SIRT1 deacetylates the RelA/p65 subunit of NF- κ B at lysine 310, leading to decreases the NF- κ B transcriptional activity, thereby reducing production of proinflammatory cytokines and anti-apoptotic genes (Yeung, F et al., 2004). This finding demonstrates that SIRT1 activity in macrophages directly

regulates immune responses and suggests that activators of SIRT1 may play an important therapeutic role in the treatment of chronic inflammatory diseases.

2.2.6 Regulation of circadian rhythm

Circadian rhythm refers to an endogenous 24-hour oscillation of any biological processes in all living entities on earth. This circadian rhythm depends on internal clocks that work in part through chromatin modification and epigenetic control of gene expression (Winjnen, H & Young, M. W, 2006). In mammals, the circadian clock is largely controlled by negative-feedback loops mediated by the heterodimeric transcription factors CLOCK-BMAL1 and their transcriptional targets, including the PER and CRY proteins that in turn directly repress CLOCK-BMAL1 activity, as well as REV-ERB and ROR nuclear receptors that control BMAL1 expression (Winjnen, H, 2009). Early studies have shown that the expression and/or activity of SIRT1 are cyclically regulated by the circadian clock. SIRT1 interacts with CLOCK-BMAL1 to directly regulate the amplitude and duration of circadian clock-controlled gene expression through deacetylation of PER2 and BMAL1 (Asher, G et al., 2008). Later discovered that the circadian regulation of SIRT1 activity is due to circadian oscillations of the cellular NAD⁺ levels (Nakahata, Y et al., 2009). It has been found that Nampt is a direct transcriptional target of CLOCK-BMAL1. Together, these studies CLOCK-BMAL1, Nampt, NAD⁺, and SIRT1, providing an important connection between physiological rhythm and cellular metabolism.

2.3 Impact of fasting and feeding on liver metabolism

The transitions between fasting and fed states are accompanied by complex changes in hepatic gene expression. The liver is a central hub for coordination of fasting-feeding transitions given its roles in maintaining blood glucose levels, processing dietary nutrients and regulating whole-body energy metabolism (Trefts et al., 2017). During fasting the liver is the target of hormones such as glucagon, which shift it into a catabolic state (Sutherland & Cori, 1951). In response, the liver takes up free fatty acids released into the circulation by adipose lipolysis to provide energy for itself and to generate ketones for use by extrahepatic tissues (Fine & Williams, 1960). It also breaks down glycogen and amino acids to generate glucose (Berg et al., 2002). In the postprandial state, signalled by insulin and the influx of dietary carbohydrate, liver suppresses the production of glucose and switches to using it as its main fuel (Rui, 2014). Excess glucose is converted into glycogen and fatty acids. Newly synthesized and dietary fatty acids are esterified to generate triglycerides, which are packaged and exported to the circulation

(Alves-Bezerra & Cohen, 2017). Transcriptional regulation is fundamental to the execution of each of these physiological responses.

2.4 Hepatic transcriptional responses to fasting and feeding

Regulation of transcription involves the coordinated action of a bevy of transcription factors, coregulators and chromatin modifying enzymes, all acting downstream from hormonal signalling pathways. Elucidating the complex metabolic changes associated with fasting and feeding and their transcriptional underpinnings is crucial for understanding both normal physiology and metabolic pathologies (Bideyan, L et al., 2021).

2.4.1 Lipid Metabolism

2.4.1.1 Regulation of fatty acid synthesis and ketogenesis

The nuclear receptor peroxisome proliferator-activated receptor α (PPAR α) sits atop a crucial node coordinating changes in hepatic lipid metabolism during fasting (Kersten et al., 1999). PPAR α governs the expression of a battery of genes that coordinates fatty acid uptake and oxidation, ketogenesis and lipid droplet dynamics during fasting.

Regulation of acyl-coA oxidase 1 (ACOX1) by PPAR α facilitates peroxisomal long chain fatty acid (LCFA) oxidation. PPAR α induces mitochondrial LCFA oxidation through up-regulation of carnitine palmitoyltransferase 1a and 2 (CPT1A and CPT2, which transport LCFA into the mitochondria), malonyl-CoA decarboxylase (which degrades the CPT1 inhibitor malonyl-CoA) and other β oxidation enzymes. PPAR α also induces ketogenesis pathway enzymes, including 3-hydroxy-3-methylglutaryl-CoA lyase (HMGCL), acetyl-CoA acetyltransferase 1 (ACAT1) and 3-hydroxy-3-methylglutaryl-CoA synthase 2 (HMGCS2) (Cheon Y et al., 2005). Additionally, PPAR α induces expression of fibroblast growth factor 21 (FGF21), a liver hormone that promotes β oxidation and ketogenesis (Potthoff et al., 2009). FGF21 contributes to the up-regulation of proliferator-activated receptor γ coactivator protein-1 α (PGC-1 α), which serves as a transcriptional coactivator of genes in LCFA oxidation and ketogenesis (Rhee et al., 2003).

Importantly, fatty acids and their derivatives are activating ligands for PPAR α and thereby help to control their own metabolism (Keller et al., 1993). During fasting, PPAR α has been shown to be activated by the influx of FFA from adipose lipolysis (Kersten et al., 1999). However, Sanderson et al., 2010 suggested that PPAR δ also activated by FFA from adipose lipolysis during fasting. SIRT1, glucocorticoid receptor (GR) and PGC-1 α are known to promote PPAR α activity during fasting (Goldstein et al., 2017) (**Figure 2.2**). Suppression of the

mechanistic target of rapamycin kinase (mTOR) signalling in fasting was found to be necessary for PPAR α ketogenic activity (Sengupta et al., 2010).

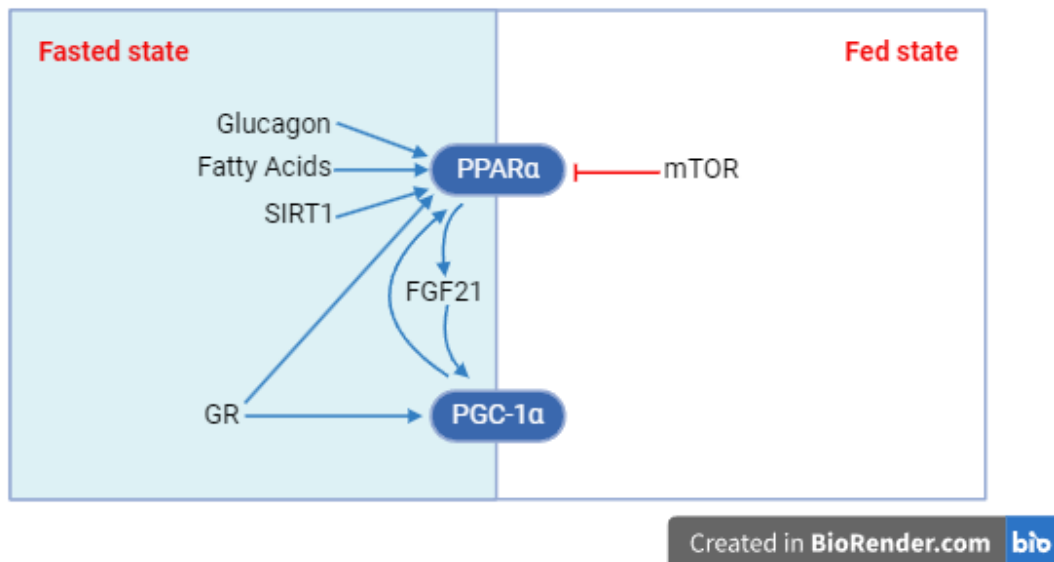


Figure 2.2: Regulation of fatty acid oxidation and ketogenesis

Transcription factors such as PPAR α and PGC-1 α are activated by glucagon, SIRT1, fatty acids and their derivatives and glucocorticoid receptor during fasting. These transcription factors induce the expression of genes that promote fatty acid oxidation and ketogenesis during fasting. (Created with BioRender.com) (Adapted from Bideyan L et al., 2021)

2.4.1.2 Regulation of lipogenesis and cholesterol synthesis

The fed state, following a meal, presents the body with a surge of nutrients, particularly carbohydrates and fats. To efficiently manage this influx, a complex regulatory network governs the synthesis of two key biomolecules: fatty acids and cholesterol. This coordinated effort ensures the body stores excess energy for later use while maintaining adequate cholesterol levels for essential functions.

Sterol regulatory element binding protein 1c (SREBP-1c) is induced in the fed state and plays a central role in coordinating lipid synthesis (Guan et al., 1997). SREBP-1c induces the transcription of multiple genes in fatty acid biosynthesis. It drives expression of ATP citrate lyase (ACLY) to make acetyl-CoA, and acetyl-CoA carboxylase α (ACC1) and FASN to convert acetyl-CoA into palmitate. Regulation of elongation of very long chain fatty acids protein 6 (ELOVL6) and stearoyl-CoA desaturase (SCD-1) by SREBP-1c facilitates the elongation and desaturation of fatty acids (Shimano et al., 1999). Regulation of fatty acid desaturases 1 and 2 (FADS1 and FADS2) by SREBP-1c further influences polyunsaturated

fatty acid (PUFA) generation. SREBP-1c also regulates the expression of genes encoding proteins linked to triglyceride synthesis, including PNPLA3, GPAM, malic enzyme and G6PD.

Insulin secretion in response to a carbohydrate-rich diet promotes both the transcription of *Srebf1* (the gene encoding SREBP-1c) and processing of immature SREBP-1c protein (Horton et al., 1998). Analysis of the *Srebf1* promoter has identified several transcription factors that contribute its insulin responsiveness, including liver x receptors (LXRs), CCAAT enhancer binding protein β (C/EBP β) and basic helix-loop-helix family member e40 (BHLHE40) (**Figure 2.3**) (Bideyan L et al., 2021).

Studies have further suggested that SREBP-1c is regulated by phosphorylation and acetylation. Phosphorylation by protein kinase A (PKA) attenuates SREBP-1c binding at lipogenic promoters (Lu & Shyy, 2006). SREBP-1c is acetylated under high-glucose conditions by histone acetyltransferase p300 (Ponugoti et al., 2010). E4 promoter-binding protein 4 (E4BP4), a transcription factor that is up-regulated during feeding which interacts with mature SREBP-1c and protects it from degradation by promoting its acetylation (**Figure 2.3**) (Tong et al., 2016).

LXR α is a nuclear receptor activated by oxysterols (Janowski et al., 1999). Anthonisen et al., 2010 suggested that glucose feeding can activate LXR via O-linked β -N-acetylglucosamine (O-GlcNAc) modification (**Figure 2.3**).

Upstream transcription factor (USF-1) is another factor important in the lipogenic response. USF-1 is necessary for the full activation of *Fasn* by feeding and insulin. USF-1 binds to the *Fasn* promoter constitutively, but its activity is modulated by post-translational modifications. USF-1 bound to the *Fasn* promoter is phosphorylated by DNA-dependent protein kinase (DNA-PK) during feeding, thereby inducing transcription (**Figure 2.3**) (Wong et al., 2009). In contrast, USF-1 has been reported to be deacetylated by histone deacetylase 9 (HDAC9) during fasting, which prevents the recruitment of activating factors (Wong et al., 2009).

Carbohydrate-responsive element-binding protein (ChREBP) is a transcription factor that induces hepatic lipogenesis in response to glucose signals. ChREBP has been shown to physically interact with hepatocyte nuclear factor 4 α (HNF4 α) on the *Fasn* promoter, facilitating its binding during feeding (Adamson et al., 2006). The *Chrebp* gene is also an LXR target, and LXR α is necessary for induction of ChREBP α expression and activity (Fan et al., 2017). Additionally, post-transcriptional modifications, especially phosphorylation by PKA and 5'-AMP-activated protein kinase (AMPK) during fasting, have been shown to

decrease ChREBP DNA binding (**Figure 2.3**) (Kawaguchi et al., 2002). In the setting of high glucose availability, xylulose-5-phosphate (Xu5P), an intermediate of the pentose-phosphate shunt, leads to the dephosphorylation of ChREBP through Xu5P-activated protein phosphatase (PP2a) (Kabashima et al., 2003).

Cholesterol biosynthesis controlled by SREBP-2 is also up-regulated in the fed state. Forkhead box protein O3 (FOXO3) cause down-regulation of the SREBP-2 pathway during fasting by recruiting SIRT6 to the promoter of *Srebf2* (the gene encoding SREBP-2) (**Figure 2.3**) (Tao et al., 2013).

There is conflicting evidence as to the role of inositol-requiring, endoplasmic reticulum-to-nucleus signalling protein 1a (IRE1a) and X-box-binding protein (XBP1) signalling in fasting and refeeding. Pfaffenbach et al., 2010 reported that mTORC1 activates IRE1a-XBP1 in the postprandial period in the context of lipogenesis.

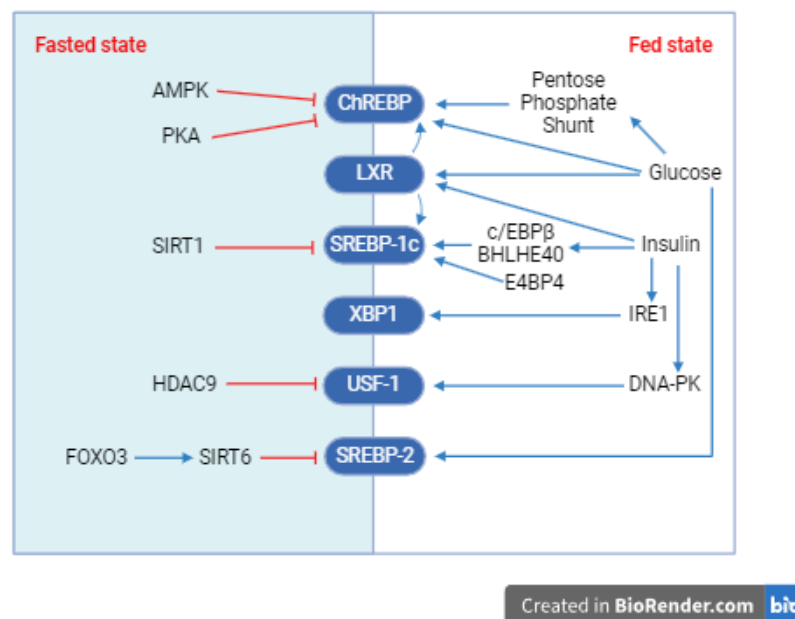


Figure 2.3: Regulation of lipogenesis and cholesterol synthesis

Transcription factors such as ChREBP, LXR, SREBP-1c, XBP, USF-1 and SREBP-2 are activated by various factors in response to feeding signals such as glucose and insulin. These transcription factors induce the expression of genes that promote lipogenesis and cholesterol biosynthesis. Some of these transcription factors are also known to be actively inhibited during fasting. (Created with BioRender.com) (Adapted from Bideyan L et al., 2021)

2.4.2 Glucose Metabolism

2.4.2.1 Regulation of glucose metabolism during fasting

CREB, cyclic AMP (cAMP) response element-binding protein (CREB) plays a dominant role in driving hepatic glucose production during fasting. CREB controls the expression of enzymes catalyzing key steps for hepatic glucose production such as glucose 6-phosphatase (G6Pase), which is necessary for both glycogenolysis and gluconeogenesis, and phosphoenolpyruvate carboxykinase (PEPCK), which is needed for gluconeogenesis from tricarboxylic acid (TCA) cycle intermediates (Quinn & Granner, 1990). The CREB homolog CREB-H is also induced during fasting and binds to CREB-regulated transcription coactivator 2 (CRTC2) to promote the expression of gluconeogenic genes (Lee et al., 2010). CREB is activated during acute fasting through phosphorylation and dephosphorylation events. A cascade involving glucagon receptor-cAMP-PKA leads to the formation of an active CREB-CREB binding protein (CBP)-CRTC2 complex (**Figure 2.4**) (Altarejos & Montminy, 2011). In contrast, in early stages of long-term fasting SIRT1 deacetylates and AMPK phosphorylates CRTC2. These modifications reduce CREB activity and facilitate a switch to FOXO1/PGC-1 α -driven gluconeogenesis (Koo et al., 2005).

FOXO1, a member of the FOXO family of transcription factors, FOXO1 regulates hepatic gluconeogenesis in both fasting and feeding. FOXO1 binds to insulin response elements in the promoters of genes involved in gluconeogenesis (Haeusler et al., 2010). During fasting, mitogen activated protein kinase (MAPK) phosphatase 3 (MPK3) dephosphorylates FOXO1, increasing its nuclear localization and activation (**Figure 2.4**) (Wu et al., 2010). Additionally in response to fasting, FOXO1 is deacetylated and thus activated by SIRT1, as well as by histone deacetylases (HDACs) that are phosphorylated by AMPK (Frescas et al., 2005) (Mihaylova et al., 2011).

PGC-1 α is a transcriptional coactivator induced by glucagon and glucocorticoid signalling that facilitates gluconeogenesis (Yoon et al., 2001). CREB induces the gene encoding PGC-1 α as the starvation progresses (**Figure 2.4**) (Herizig et al., 2001). SIRT1 deacetylates PGC-1 α during fasting, thereby increasing its activity (Rodgers et al., 2005). During fasting, PGC-1 α interacts with several hepatic transcription factors, including FOXO1 and the nuclear receptors HNF4 α , PPAR α and GR (Yoon et al., 2001).

Glucocorticoid Receptor (GR) is activated by binding to stress-related glucocorticoid hormone ligands during fasting (Opher et al., 2004). GR induces the expression of gluconeogenic genes

such as *Pck1* (Cassuto et al., 2005). Nuclear transcription factor Y (NF-Y) and nuclear factor κ b subunit 2 (NF- κ B2) have also been suggested to respond to glucagon in fasting and induce gluconeogenesis (Zhang et al., 2019). The bile acid receptor FXR, induced by PKA and FOXA1, has also been reported to promote gluconeogenic genes (Ploton et al., 2018). In addition to its role in fasting-induced fatty acid oxidation, PPAR α also affects the expression of genes linked to gluconeogenesis, glycerol metabolism and glycogen synthesis (Kersten, 2014).

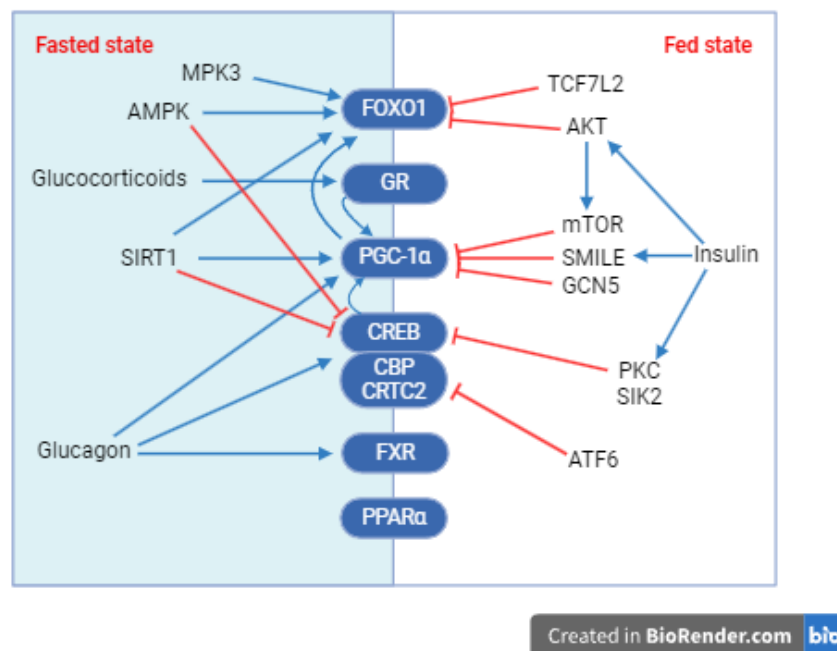


Figure 2.4: Regulation of gluconeogenesis and glycogenolysis

Transcription factors such as FOXO1, GR, PGC-1 α , CREB, PPAR α , and FXR are activated by glucagon, AMPK, SIRT1, and glucocorticoids during fasting. These transcription factors induce the expression of genes that promote gluconeogenesis and glycogenolysis. This switch is crucial in maintaining blood glucose levels during fasting. There is evidence for cross talk between these factors, one inducing the expression of another. Some of these transcription factors are also known to be actively inhibited by insulin signalling in response to feeding. (Created with BioRender.com) (Adapted from Bideyan L et al., 2021)

2.4.2.2 Regulation of glucose metabolism during feeding

ChREBP is consistent with its regulation by dietary glucose which induces genes linked to glycolysis. ChREBP is necessary for the glucose-dependent induction of pyruvate kinase (PKLR), which catalyzes the last step of glycolysis (**Figure 2.5**) (Rufo et al., 2001). Loss of ChREBP in mice decreases glycolysis at the pyruvate kinase and glucose-6-phosphatase steps

and consequently increases liver glycogen content (Iizuka et al., 2004). During feeding, interleukins 6 and 13 (IL6 and IL13) activate signal transducer and activator of transcription 3 (STAT3) (Stanya et al., 2013), which represses gluconeogenic genes such as *Pck1* and *G6pase* (Ramadoss et al., 2009). Additionally, hypoxia inducible factor 2 α (HIF2 α) is activated by hypoxia in postprandial liver, where it attenuates glucagon signalling and gluconeogenesis together along with aryl hydrocarbon receptor nuclear translocator (ARNT) (Ramakrishnan et al., 2016). Nr5a2 (also known as LRH-1) plays a role in postprandial glycolysis and glycogen synthesis by stimulating *Gck* expression (Oosterveer et al., 2012) and postprandial uptake of bile acids activates FXR to support glycogen synthesis (Massafra & Van Mil, 2018).

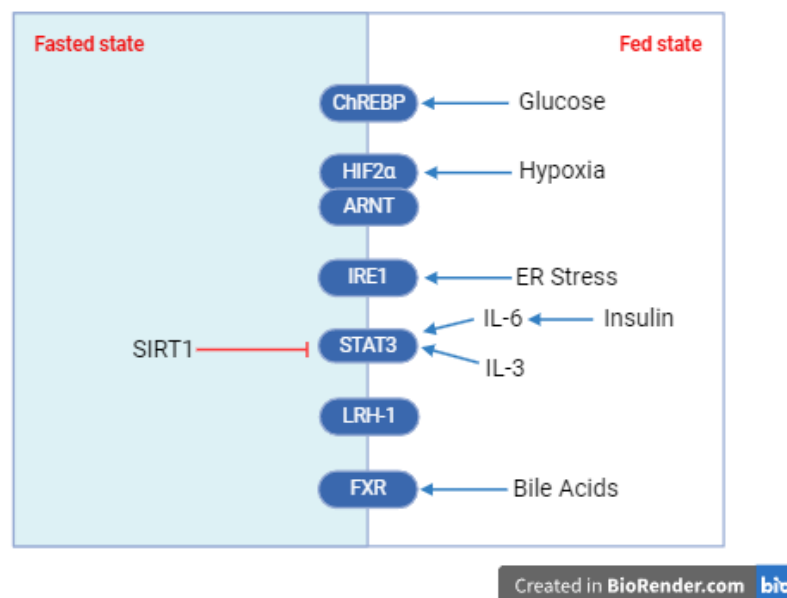


Figure 2.5: Regulation of glycolysis and glycogen synthesis

Transcription factors such as ChREBP, HIF2 α -ARNT, IRE1, STAT3, LRH-1, and FXR are activated by various factors in response to feeding such as glucose and insulin. These factors induce the transcription of genes that promote glycolysis and glycogen synthesis. In response to an increase in available glucose and insulin, energy metabolism switches to using glucose as fuel and replenishes glycogen stores. (Created with BioRender.com) (Adapted from Bideyan L et al., 2021)

2.5 SIRT1 in lipid and glucose metabolism

SIRT1 modulates cellular metabolism through deacetylation of a diverse array of target protein, with a particular focus on regulating lipid and glucose homeostasis (**Table 1.3.2**) (Ye, X et al., 2017).

2.5.1 Lipid metabolism

During fasting/starvation, free fatty acids are released from adipose tissue and oxidized (β -oxidation) to acetyl-CoA to produce ATP. In the fed condition, fatty acids are synthesized from acetyl-CoA in the liver (lipogenesis) and transferred to adipocytes for storage. Peroxisome proliferator activated receptor α (PPAR α) is a key transcription factor for fatty acid oxidation (β -oxidation). Proliferator-activated receptor- γ coactivator 1 α (PGC-1 α), a coactivator of PPAR α , is a direct substrate of SIRT1 leads to its activation (**Figure 2.6 A**). Thus, SIRT1 regulates fatty acid oxidation-related genes, including medium chain acyl-CoA dehydrogenase (*Mcadh*), acyl CoA oxidase (*Aox*), and enoyl-CoA hydratase/3-hydroxyacyl CoA dehydrogenase (*Ehhadh*), through the activation of PGC-1 α (Purushotham et al., 2009). Sterol regulatory element-binding protein (SREBP)-1c is a key lipogenic transcription factor that regulates the expression of multiple target genes, including fatty acid synthase (*Fasn*), and elongation of very long-chain fatty acids-like 6 (*Elovl6*). SIRT1 deacetylates and inhibits SREBP-1c activity in the liver (Ponugoti et al., 2010) (**Figure 2.6 B**). Therefore, hepatic SIRT1 seems to stimulate fat oxidation and inhibit fat synthesis.

Liver X receptor (LXR) regulates the expression levels of ATP-binding cassette transporter A1 (*Abca1*) and *Abcg1*, which mediate cholesterol efflux. Thus, LXR plays an important role in cholesterol transport from peripheral tissues to the liver (reverse cholesterol transport) via high density lipoprotein-cholesterol biogenesis. SIRT1 deacetylates and increases LXR activity, leading to the enhancement of reverse cholesterol transport (Li et al., 2007) (**Figure 2.6 C**). Farnesoid X receptor (FXR) is a nuclear bile acid receptor that regulates the expression of bile acid transporters, such as *Abcb 11*/bile salt export pump (*Bsep*). Acetylation of FXR inhibits its activity, and SIRT1 increases the binding of FXR to promoter chromatin through the deacetylation of FXR (Kemper et al., 2009) (**Figure 2.6 D**).

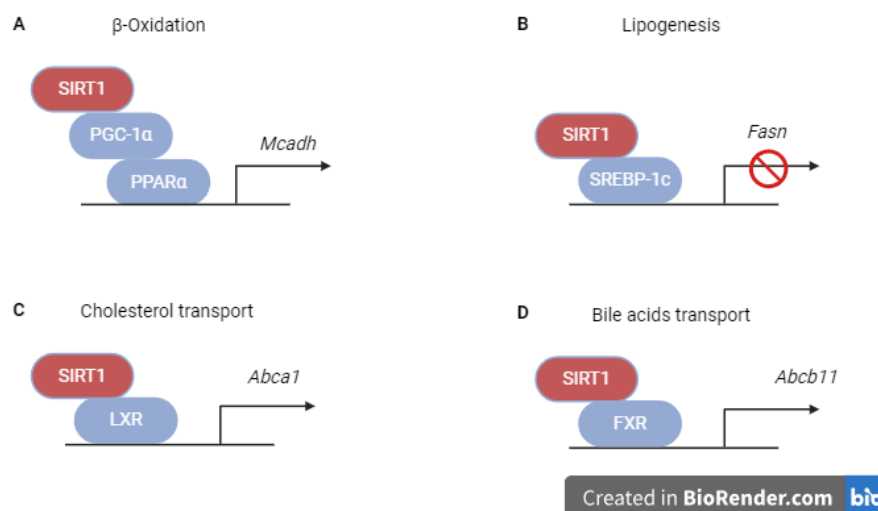


Figure 2.6: Transcriptional regulation of lipid metabolism related genes by SIRT1 in liver.

(A) and (B) SIRT1 enhances β -oxidation via deacetylation of PGC-1 α /PPAR α , while SIRT1 attenuates lipogenesis by inhibiting SREBP-1c. (C) and (D) SIRT1 activates reverse cholesterol transport by deacetylating LXR and increases the export of bile acids by increasing the expression of transporters via FXR.

2.5.2 Glucose metabolism

SIRT1 positively controls the gluconeogenic genes glucose-6-phosphatase (*G6pc*) and phosphoenolpyruvate carboxykinase (*Pck1*) in the liver in response to fasting signals through the deacetylation and activation of PGC-1 α and FOXO1 (Rodgers et al., 2005). But it has a dual but controversial role in the regulation of gluconeogenesis under the condition of calorie restriction. In early stages of long-term fasting, SIRT1 deacetylates CREB-regulated transcription co-activator 2 (CRTC2), leading to CRTC2 degradation and thus decreases hepatic glucose production (Yi L et al., 2008) (**Figure 2.7 A**). On the contrary, in the prolonged phase of fasting, SIRT1 activates FoxO1 and PGC-1 α to increase hepatic glucose production. SIRT1 activation renders FoxO1 immobile within the nuclear compartment and promotes FoxO1-dependent transcription of genes important for hepatic glucose production (Wang F & Tong Q, 2009) (**Figure 2.7 B**). Also, SIRT1 interacts with and deacetylates PGC-1 α at specific lysine residues in a NAD⁺-dependent manner and activates gluconeogenic genes and hepatic glucose output through PGC-1 α (JT, R., 2005) (**Figure 2.7 C**).

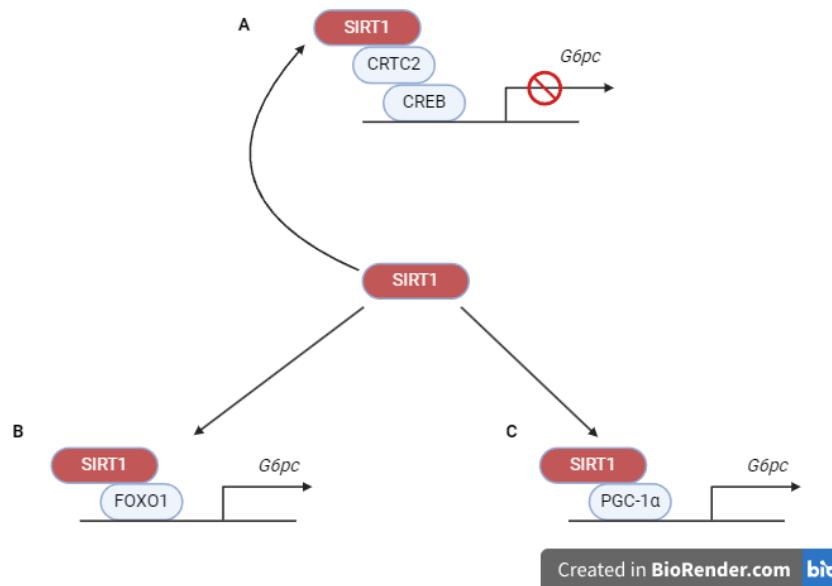


Figure 2.7: Transcriptional regulation of glucose metabolism-related genes by SIRT1 in the liver.

(A) In the early stage of long-term fasting, SIRT1 deacetylates CRTC2, which causes CRTC2 degradation and inhibits gluconeogenesis genes, and at the same time (B) and (C) SIRT1 activates PGC-1α and FOXO1 by deacetylating them and turn on genes necessary for response to long-term fasting.

2.6 Hepatocyte specific deletion of SIRT1

PPARα is a lipid-sensing member of the nuclear receptor superfamily that regulates systemic fatty acid metabolism. Under normal physiological conditions in mice, PPARα levels in the liver peak in the late afternoon and decrease immediately after food intake (Yang et al., 2006). Activation of PPARα by fatty acids and metabolites leads to transcriptional activation of various target genes involved in fatty acid oxidation, which are required for the normal adaptive response to starvation. Consequently, mice lacking PPARα accumulate excessive triglyceride in the liver and become hypoketonemic during fasting (Hashimoto et al., 2000). SIRT1 LKO mice displayed reduced expression of several PPARα target genes after overnight fasting. Interestingly, the expression of PGC-1α, a transcription cofactor known to activate PPARα was also significantly lower in SIRT1 LKO mice (Purushotham et al., 2009).

In addition to fatty acid oxidation, PGC-1α also stimulates hepatic gluconeogenesis in response to fasting (Herzig et al., 2001). The decreased coactivation activity of PGC-1α in SIRT1 liver knockout mice suggests that gluconeogenesis may be impaired. However, Glucose-6-phosphatase (*G6Pase*), phosphoenol pyruvate carboxykinase (*PEPCK*) gene expression and fasting glucose levels are reportedly normal in hepatocyte-specific SIRT1 knockout mice, given the fact that SIRT1 also deacetylates and represses CRTC2. Therefore, the net effect of

loss of SIRT1 on gluconeogenesis is determined by the complex compensatory patterns of multiple factors (Purushotham et al., 2009).

FXR is a nuclear bile acid receptor that regulates the expression of bile acid transporters, such as *Abcb11*/bile salt export pump (*Bsep*). Acetylation of FXR inhibits its activity and SIRT1 increases the binding of FXR to promoter chromatin through the deacetylation of FXR. Hepatocyte-specific deletion of SIRT1 leads to derangements in bile acid metabolism due to the reduced expression of bile acid transporters and decreased HNF1 α recruitment to the FXR promoter and reduced expression of FXR, leading to decreased transport of biliary bile acids and phospholipids and increased incidence of cholesterol gallstones (Purushotham et al., 2012).

Overall, the studies of SIRT1 knockout in hepatocytes suggests that SIRT1 in liver cells plays an important role in both lipid and glucose metabolism. Deleting SIRT1 disrupts these processes and can lead to liver problems and potentially other metabolic issues.

Despite the widespread expression of SIRT1, it exhibits tissue-specific functions, suggesting potential regulatory mechanisms beyond simple gene expression levels. Thus, it is necessary to understand how SIRT1 interacts with different target proteins can explain its diverse effects. A key challenge was identifying regions of SIRT1 that determine which proteins it binds and modifies. So Deota S et al., 2017 discovered a new isoform of SIRT1 called SIRT1- Δ E2 which lacks a specific part (exon 2) present in the standard form of SIRT1-FL. And they showed that the missing exon 2 (E2 domain) in SIRT1- Δ E2 played a crucial role in how SIRT1 interacts with other proteins.

Thus, to investigate the liver-specific functions of SIRT1- Δ E2, we analysed the mouse lines that lacks Δ E2 of SIRT1 specifically in liver. The rationale behind this liver specific knockout was to examine how SIRT1- Δ E2 interacts with the proteins, affects gene expression and modulates the liver metabolism.

The objective of this project was to elucidate the functional role of the SIRT1- Δ E2 isoform in liver physiology, with a particular focus on its impact on metabolism compared to the full-length SIRT1 (WT).

CHAPTER 3

MATERIALS AND METHODS

3. Materials and Methods

3.1 Materials

3.1.1 Chemical Reagents

The chemical reagents and kits used in various methods are mentioned in the following section.

Table 3.1: Reagents used for genotyping

Reagents	Specifications	Producer information
KAPA Mouse Genotyping Kit	Catalogue no. KK7302	Sigma-Aldrich®
2x KAPA2G Fast Genotyping Mix with dye	Master mix containing all necessary components	Sigma-Aldrich®
KAPA Express Extract 1U/μL	Thermostable protease	Sigma-Aldrich®
10x KAPA Express Extract Buffer	Lysis buffer	Sigma-Aldrich®

Table 3.2: Reagents used for lysate preparation

Reagents	Specifications	Producer information
cOmplete™, EDTA-free protease Inhibitor Cocktail	COEDTAF-RO	Roche
phosSTOP™	PHOSS-RO	Roche
Phenylmethanesulfonyl fluoride (PMSF)	P7626	Sigma-Aldrich®

Table 3.3: Reagents used for BCA assay

Reagents	Identifier	Producer information
Bovine serum albumin	160069	MP Biomedicals
Bicinchoninic Acid solution (BCA)	B9643	Sigma-Aldrich®

Table 3.4 Reagents used for SDS-PAGE

Reagents	Identifier	Producer information
20% SDS	ML007	Himedia
Acrylamide/Bis acrylamide	ML037	Himedia
APS	248614	Sigma-Aldrich®
TEMED	76320	USB
Tris	194855	Mp Biomedicals

Table 332.5: Reagents used for western blot

Reagents	Identifier	Producer information
PVDF Membrane	IPVH00010	Millipore
Skim milk powder	GRM1254	Himedia
Tween-20	TC287	Himedia
Enhanced chemiluminescence - Pico	34080	Thermo Scientific™
Enhanced chemiluminescence - Femto	34095	Thermo Scientific™

Table 3.6 Antibodies used for western blot

Primary Antibodies	Identifier	Producer Information
SIRT1	07-131	Millipore
PGC-1 α	SC13067	Santacruz
AKT	9272S	Cell Signalling
pAKT	9814S	Cell Signalling
FOXO1	2880S	Cell Signalling
pFOXO1	84192S	Cell Signalling
CREB	9197S	Cell Signalling
pCREB	4276P	Cell Signalling
Secondary Antibodies	Identifier	Producer Information
Anti-Rabbit IgG-Peroxidase	A0545	Sigma-Aldrich
Anti-Mouse IgG-Peroxidase	A9044	Sigma-Aldrich

Table 3.7: Reagents used for isolation of RNA

Reagents	Identifier	Producer information
TRIzol	15596018	Invitrogen™
Chloroform	Q12305	Qualigens
Isopropanol	DG1P710844	Emparta®
EtOH	32221	Honeywell
DEPC treated water	AM9915G	Invitrogen™

Table 3.8: Reagents used for cDNA synthesis

Reagents	Identifier	Producer information
Random hexamers (50 μ M)	10777019	Invitrogen™
dNTP Mix	652400021730	GeNei™
DTT	578517	Sigma-Aldrich®
Superscript-IV RT kit	18090200	Invitrogen™
RnaseOUT™ Recombinant Ribonuclease Inhibitor	10777019	Invitrogen™

Table 3.9: Reagents used for qPCR

Reagents	Identifier	Producer information
Luna® Universal qPCR Master Mix	M3003	New England Biolabs
Ultrapure Distilled water	10977015	Invitrogen™
6x DNA loading buffer	2071	GeNei™

3.1.2 DNA molecular size marker

GeneRuler DNA 1 kb plus ladder from GeNei™, with fragments of size 10000, 8000, 6000, 5000, 4000, 3000, 2500, 2000, 1815, 1500, 1185, 1000, 900, 800, 700, 600, 500, 400, 300, 200 and 100 with 600 bp, 1000 bp and 3000 bp spiked as reference point for easy detection.

3.1.3 Prestained protein ladder

The Blu12 Prestained Protein Ladder from Bio-Helix is a combination of 12 pre-stained proteins with molecular weights from 11 to 245 kDa. The 12 recombinant proteins are covalently couples with blue chromophore, while 1 green band at 25kDa and a red band at 75 kDa serve as reference bands.

3.2 Methods

3.2.1 Generation of liver specific SIRT1-ΔE2 mouse models (EC171C)

The Cre-lox system is a powerful tool for generating tissue-specific gene knockout mice. A liver-specific SIRT1-ΔE2 knockout mouse model was generated. Albumin-Cre recombinase strain mice were first crossed with floxed mice harboring loxP sites flanking exon 2 of the SIRT1 gene. The resulting offspring (F1 generation) were heterozygous for the loxP sites and Albumin-Cre allele. Subsequently, these F1 mice were interbred. In the F2 generation, approximately 25% of the pups were expected to be homozygous for the floxed SIRT1-ΔE2

allele and Albumin-Cre recombinase. The mice homozygous for the loxP sites and Albumin-Cre are the SIRT1-ΔE2 mice models (**Figure 3.1**).

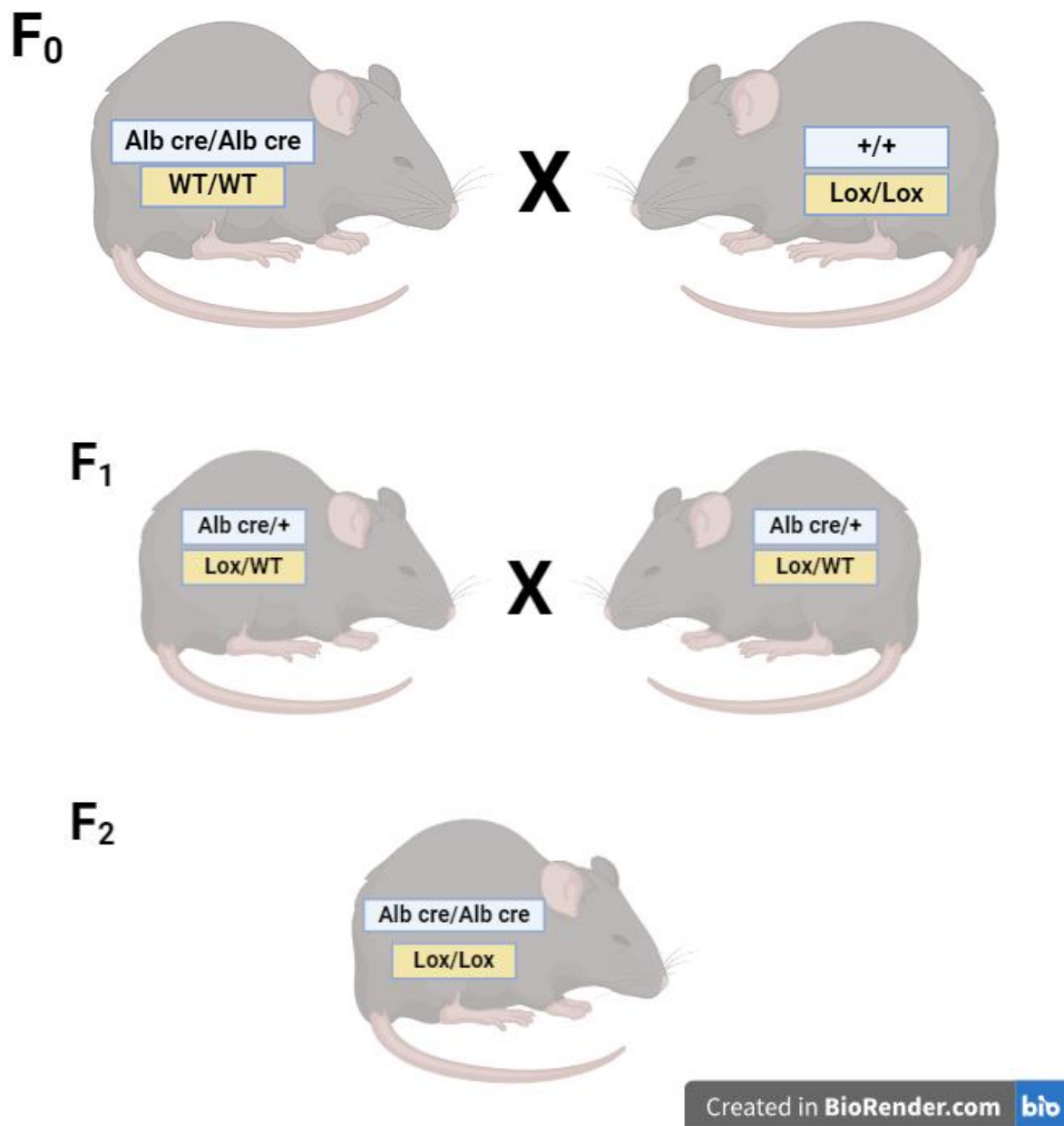


Figure 3.1: Schematic representation of generation of liver specific SIRT1-ΔE2 mice
About 25% of the offspring in F₂ generation will be homozygous for the loxP flanked allele and Albumin Cre recombinase.

3.2.2 Tail clip digestion

To make sure that they are the expected genotype, genomic DNA were extracted from those animals' tail clips by tail clip digestion. 1 mm tail clips were collected from those animals. The reagents mentioned in the **Table 3.10** were mixed and the reaction mixture was added to the tail clips tubes and incubated at 75° C for 15 minutes. After digestion, the tail clips tubes were incubated at 95° C for 5 minutes for the inactivation of enzymes. After inactivation, the samples were spun at room temperature and diluted for 50µl in 1:10 ratio.

Table 3.10: Reaction mixture for tail clip digestion

Reagents	Volume (µL)
10x KAPA Express Extract Buffer	10
KAPA Express Extract 1U/µL	2
Double autoclave H ₂ O	Final reaction volume to 100
Total volume	100

3.2.3 Designing of Primers

The primers used to amplify Albumin-Cre wildtype and mutant, E2lox/lox for genotyping (**Table 3.11**), Actin forward primer and reverse primer for qPCR (**Table 3.12**), and SIRT1 E1 internal forward, E1-E3 junction and E5 reverse (**Table 3.13**) were designed by Arushi S, a PhD student in the lab using the NCBI primer BLAST.

Table 3.11: Primers used for Genotyping

Primers	Sequences
Albumin-Cre Forward Primer 1	TGCAAACATCACATGCACAC
Albumin -Cre Forward Primer 2	GAAGCAGAAGCTTAGGAAGATGG
Albumin-Cre Reverse Primer	TTGGCCCCTTACCATAACTG
E2 lox Forward Primer	AACAAACCTGAAACAAACCT
E2 lox Reverse Primer	CAGTCCCTAACACGTTTTGT

Table 3.12: Primers used for qPCR

Primers	Sequences
Actin Forward Primer	CCTCCCTGGAGAAGAGCTATGA
Actin Reverse Primer	GCACTGTGTTGGCATAGAGGTC

Table 3.13: Primers used for E2 knockout confirmation

Primers	Sequences
SIRT1 E1 Internal Forward Primer	CTTCGACGACGACGAGGGCGAGGA
E1-E3 Junction Forward Primer	CAGCGATCGGCTACCGAGGCCAT
E5 Reverse Primer	ACGGGCCCTCGAGCATGACACTGAAGGATCCTTTGG

3.2.4 Genotyping by PCR

Extracted genomic DNA from the generated animals' tail clips were subjected to genotyping to confirm that they were the expected genotype. Two sets of genotyping PCR was done, 1. Albumin-Cre and 2. E2lox/lox. Specific primers were designed by Arushi S, a PhD student in the lab using NCBI primer BLAST were used to amplify Albumin-Cre and LoxP sites. The PCR reaction mixture for Albumin-Cre was prepared by combining the necessary reagents mentioned in the **Table 3.14** and the PCR amplification was carried out using the conditions outlined in **Figure 3.2**. And the PCR mixture for E2Lox was prepared by combining the necessary reagents mentioned in the **Table 3.16** and the PCR amplification was carried out using the conditions outlined in **Figure 3.3**.

Table 3.14: Reaction mixture for Albumin-Cre Genotyping PCR

Reagents	Volume (μL)
2x KAPA2G Fast Genotyping Mix with dye	6.25
Albumin-Cre Forward Primer 1	0.625
Albumin-Cre Forward Primer 2	0.625
Albumin-Cre Reverse Primer	0.625
qH ₂ O	3.37
Template	2

Table 3.15: Thermal cycles for Albumin-Cre Genotyping PCR amplification

Cycle Step	Temperature (°C)	Time (s)	Cycles
Initial Denaturation	94	120	1
Denaturation	94	20	10
Annealing	65	15	
Extension	68	10	
Denaturation	94	15	28
Annealing	60	15	
Extension	72	60	
Final Extension	72	180	1
	12	Hold	

Table 3.16: Reaction mixture for E2lox/lox Genotyping PCR

Reagents	Volume (µL)
2x KAPA2G Fast Genotyping Mix with dye	6.25
E2 lox Forward Primer	0.6
E2 lox Reverse Primer	0.6
qH ₂ O	4.05
Template	2

Table 3.17: Thermal cycles for E2lox/lox Genotyping PCR amplification

Cycle Step	Temperature (°C)	Time (s)	Cycles
Initial Denaturation	96	180	1
Denaturation	96	30	35
Annealing	58	30	
Extension	72	60	
Final Extension	72	600	1
	4	Hold	

For the PCR reaction, an Eppendorf[®] Multiplex Thermocycler was utilized to facilitate the temperature cycling required for amplification. The full PCR reaction was carried out using a reaction volume of 13.5µL for both Albumin-Cre and E2lox/lox. After the PCR amplification, the resulting products were electrophoresed on a 2% agarose gel for Albumin-Cre and 1.5% agarose gel for E2lox/lox.

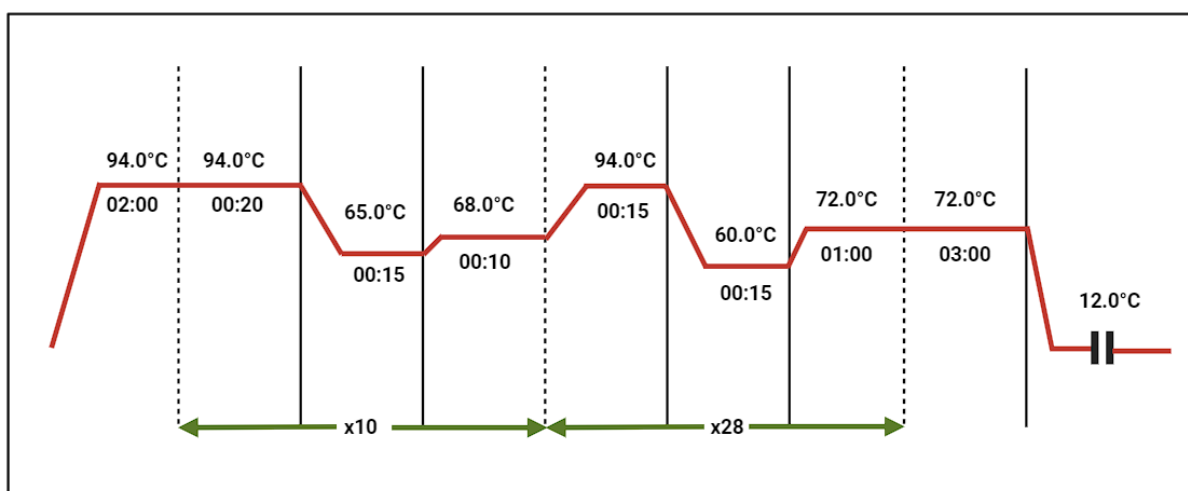


Figure 3.2: Schematic representation of Albumin-Cre Genotyping PCR parameters employed during execution

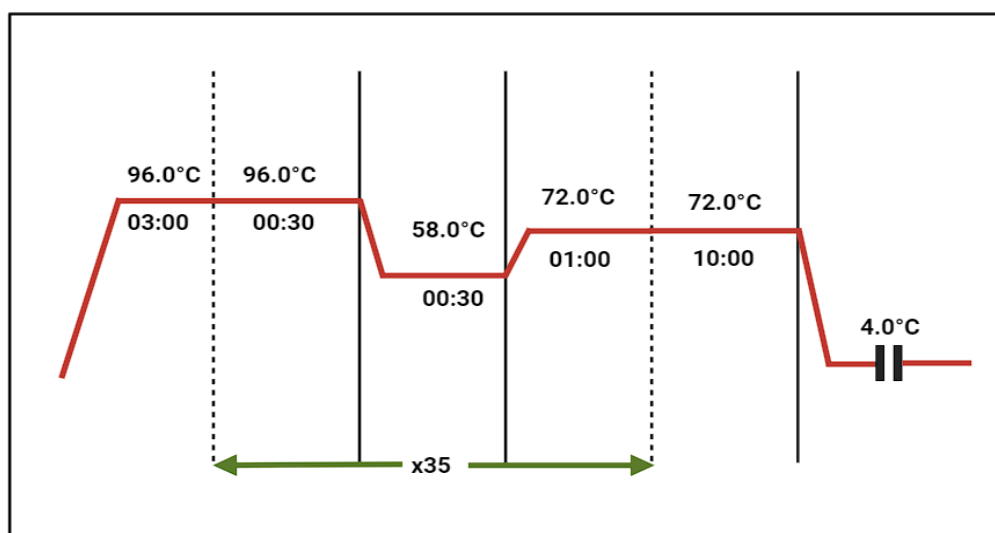


Figure 3.3: Schematic representation of E2lox/lox Genotyping PCR parameters employed during execution

3.2.5 Preparation of Lysate

To prepare lysates from the liver tissues, RIPA buffer with the inhibitors were aliquoted as 200µL per sample as mentioned in the **Table 3.18**. By placing the tissue pieces in cold condition, the aliquoted buffer was added 200µL per sample and homogenised with pestle. The buffer disrupts cell membranes and solubilizes proteins. The homogenate was then incubated on ice for 15 minutes to ensure complete lysis. After the incubation, the homogenate was centrifuged for 15 minutes in 13000 rpm at 4° C to remove cell debris and isolate the protein-containing supernatant. The lysate was collected and transferred to fresh MCTs in cold condition. A small amount of the supernatant was reserved for protein concentration

determination using a BCA assay. The remaining supernatant was mixed with 4x Laemmli sample buffer at a ratio to achieve a final 1x Laemmli concentration and incubated in 95° C for 10 min. After the incubation, the lysates were stored in -20° C.

Table 3.18: Aliquot volumes for RIPA buffer with the inhibitors

Components	Volume (μL)	Final Concentration
25x PIC	12	1.5x
25x phosSTOP	12	1.5x
PMSF	2	1x
RIPA Buffer	Final reaction volume to 200	
Total volume	200	

3.2.6 BCA Assay

BCA assay was conducted to quantify protein concentration in the prepared lysates. First, BCA working reagents was prepared by mixing 50 parts of BCA reagent A (50mg/mL of bicinchoninic acid) with 1 part of BCA reagent B (4% cupric sulfate solution in 0.4N sodium hydroxide). Then a series of BSA standards with known concentration ranging from 0 - 1000μg/μL was prepared in duplicates with distilled water in separate wells of a flat-bottomed 96-well microplate. The protein samples were also likely diluted to a specific concentration range in duplicates. Then 200μL of working BCA reagent was added to each well of the plate. Then the plate was taken to measure the absorbance at 562nm using a microplate reader to plot a standard curve using the absorbance values of the BSA standards. Using the standard curve, the protein concentration across the samples were calculated.

3.2.7 Western Blot Analysis

3.2.7.1 SDS-PAGE

To confirm the knockout of E2 domain in protein level, western blot analysis was done. In the first step of a western blot, SDS-PAGE was performed to separate proteins based on their size by denaturing them and giving them uniform negative charge. For this, the glass plates and spacers of the gel casting unit were cleaned with deionized water and ethanol, and assembled the plates with the spacers on a stable, even surface. Then, 6% resolving gel solution was prepared for 10ml by dissolving the reagents mentioned in **Table 3.19**. The gel solution was poured in the plates assembled with spacers. To maintain an even and horizontal resolving gel

surface, the surface was overlayed with isopropanol. The gel was allowed to set for about 20-30 minute at room temperature. Then, stacking gel solution was prepared for 4ml by dissolving the reagents mentioned in **Table 3.20**. By discarding the overlayed isopropanol on the resolving gel, the stacking gel solution was added until it overflows. The comb was inserted immediately ensuring no air bubbles are trapped in the gel or near the wells and the gel was allowed to set for about 20-30 minutes at room temperature. The lysate samples were taken from -20° C and boiled at 95° C for 5 minutes and centrifuged at room temperature. Adequate 1x SDS running buffer was added to the tank and 30µg of proteins from lysates were loaded in the gel. The electrophoresis was performed along with the protein ladders at 90V initially. When the lysates pass the stacking/enters the resolving gel, it was changed to 120V.

Table 3.19: Components for 6% Resolving Gel

Reagents	Volume (mL)
Water	5.3
Acrylamide	2
1.5 M Tris (pH 8.8)	2.5
100g/L SDS	0.1
100g/L APS	0.1
TEMED	0.008
Total Volume	10

❖ TEMED must be the last ingredient added

Table 3.20: Components for Stacking Gel

Reagents	Volume (mL)
Water	2.7
Acrylamide	0.67
1.0 M Tris (pH 6.8)	0.5
100g/L SDS	0.04
100g/L APS	0.04
TEMED	0.004
Total Volume	4

❖ TEMED must be the last ingredient added

3.2.7.2 Membrane Transfer

To transfer the electrophoresed proteins from the gel to membrane, sufficient transfer buffer (1x) was prepared by mixing the reagents mentioned in **Table 3.21** and kept in cold condition before using. After the gel electrophoresis was done, the gel was removed from its cassette and trimmed the stacking gel and wells. The gel was immersed in transfer buffer. The PVDF membrane was prepared by wetting it with ethanol for 15 seconds and carefully placed in Milli-Q[®] water and soaked for 2 minutes and placed in transfer buffer. Then, the transfer stack was assembled in the transfer buffer. By opening a cassette holder, a foam pad was placed on one side of the cassette. One sheet of filter paper was placed on top of the pad. The gel was placed on top of the filter paper and the membrane was placed on top of the gel. By placing a second sheet of filter paper on top of the stack and a foam pad on top of the filter paper, the cassette holder was closed. To ensure an even transfer, air bubbles were removed between the layers by a blot roller over the surface of each layer in the stack. The cassette holder was placed in the transfer tank so that the gel side of the cassette holder is facing the cathode (-) and the membrane side is facing the anode (+). Adequate buffer was added into the tank to cover the cassette holder. A cool pack was placed in the transfer tank. The tank was connected to the power outputs and the system was turned on for 1.30 hours at 100V.

Table 3.21: Composition of Transfer Buffer

Reagents	Amount	Final concentration	Final Volume (L)
Tris-base	60.6 g	10x	2
Glycine	288 g		
Milli-Q [®] water	Final volume to 2 L		
10x Transfer buffer	100 mL	1x	1
Crude EtOH	200 mL		
Milli-Q [®] water	700 Ml		

3.2.7.3 Blocking

After the transfer gets completed, the membrane was placed in 5% milk, which was prepared by dissolving the 4 grams of skimmed milk powder by making up the volume to 80mL by 1x TBST. The composition of 1x TBST is shown in **Table 3.22**. The membrane was completely

soaked and kept in a gentle shake for 1 hour. Then, the membrane is washed in 1x TBST for 15 minutes for three times.

Table 3.22: Composition of 1x TBST

Reagents	Volume (mL)
Milli-Q [®] water	950
1x TBS	50
Tween solution	1
Total Volume	1000

3.2.7.4 Antibody Incubations

To analyse SIRT1 and β -Tubulin, the membrane was cut along 135-100 kDa marker for SIRT1 and 48-35 kDa marker for β -Tubulin into two linear membranes. The blots were sealed in separate primary antibodies for SIRT1 and β -Tubulin mentioned in **Table 3.6** and kept in cold room for 12 hours in a gentle shaker. After 12 hours, the blots were transferred to 1x TBST for three-time wash, each for 15 minutes. Then, the SIRT1 blot was placed in 1:6000 ratio of Anti-Rabbit IgG-Peroxidase secondary antibody in 5% milk and β -Tubulin in 1:6000 ratio of Anti-Mouse IgG-Peroxidase secondary antibody in 5% milk, and incubated in gentle shake for 1.5 hours. After the incubation, the blots were transferred to 1x TBST for three-time wash, each for 15 minutes.

3.2.7.5 Chemiluminescent Detection

To visualize the targeted protein, chemiluminescence detection kit from Thermo Scientific was used and visualized under Amersham Imager 600, which captures the image at optimum exposure time to capture the signal and also captures the image at multiple times by adding the exposure time. To capture the image Pico A and B from the kit was added in 1:1 ratio to the membrane and kept in the imager. If the signal were very weak in the blots, Femto A and B were added in 1:1 ratio to the blots to capture the image.

3.2.8 Isolation of RNA by TRIzol

To confirm the knockout of E2 domain in mRNA level, RNA was isolated from the liver tissues by TRIzol method. By keeping the samples in ice, 500 μ L of TRIzol was added to the samples and homogenised using pestle. After homogenization, the samples were incubated at room temperature for 5 minutes to allow complete dissociation of nucleoprotein complexes. 100 μ L

of chloroform was added to the samples and gently inverted them 5 to 6 times to ensure proper mixing but avoiding creating emulsions. The samples were centrifuged at 13000 rpm for 15 minutes in 4° C. This centrifugation will separate the mixture into three distinct layers, in which upper aqueous phase contains RNA; interphase contains DNA and denatured proteins and lower organic phase contains organic solvents. From which, upper aqueous layer was transferred to a fresh RNase-free MCTs by avoiding disturbing the interphase or lower organic phase. 100 µL of chloroform was added again to the aqueous layer and centrifuged at 13000 rpm for 15 minutes in 4° C. From which, upper aqueous layer was transferred to a fresh RNase-free MCTs by avoiding disturbing the interphase. 0.5 volume of initial volume of isopropanol was added to the isolated aqueous phase and incubated at -20° C for minimum 2 hours. The sample was then centrifuged at 13000 rpm for 15 minutes in 4° C. A white RNA pellets would be formed at the bottom of the tube. The supernatant was discarded carefully without disturbing the pellets. 70% EtOH was prepared by dissolving the reagents mentioned in the **Table 3.23** and added to the pellets for washing the salts out by centrifuging them in 12000 rpm for 10 minutes at 4° C. the supernatant was discarded completely and briefly spinned the tube to remove any residual EtOH. RNA pellets were kept to dry in 37-40° C. Overdrying can make RNA difficult to re-suspend. Then the RNA pellets were resuspended in DEPC water and incubated the tube in 42° C for 10 min. The resulting isolated RNA was electrophoresed on a 1.5% (w/v) agarose gel. The isolated RNA was stored in -20° C.

Table 3.23: Composition of 70% EtOH

Reagents	Volume (µL)
100% EtOH	350
DEPC water	150
Total Volume	500

3.2.9 Synthesis of cDNA

cDNA was synthesized from the isolated RNA using SSIV RT kit from Invitrogen™. 1 µg of RNA samples were added to the q.H₂O for a total of 12.4 µL. Reaction mixture A was prepared by adding the components mentioned in **Table 3.24**. 2 µL of reaction mixture A was added to the samples tubes and incubated at 65° C for 5 minutes to anneal primer to template RNA. Flash freeze the samples on ice for at least 2-3 minutes. Reaction mixture B was prepared by adding the components mentioned in **Table 3.25**. 5.6 µL of reaction mixture B was added to

the RNA samples and incubated at 23° C for 10 min. After this incubation, the combined reaction mixture was incubated again at 55° C for 10 minutes. Finally, to inactivate the reverse transcriptase, the combined reaction mixture was incubated at 80° C for 10 minutes. Then the synthesized cDNA from the samples were briefly centrifuged at room temperature and diluted as 1:10 with q.H₂O.

Table 3.24: Reaction Mixture A for cDNA synthesis

Reagents	Volume (μL)
Random hexamers	1
10mM dNTP mix	1

Table 3.25: Reaction Mixture B for cDNA synthesis

Reagents	Volume (μL)
5x SSIV Buffer	4
100mM DTT	1
SuperScript®IV Reverse Transcriptase (200U/ μL)	0.3
RNaseOUT™ Recombinant RNase Inhibitor	0.3

3.2.10 Quantitative PCR

To ensure the good quality of synthesized cDNA, qPCR was done for Actin. Specific primers were designed to amplify Actin as mentioned in **Table 3.12**. The qPCR reaction mixture was prepared by combining the necessary reagents mentioned in **Table 3.26**, and the qPCR amplification was carried out in duplicates with one negative control

Table 3.26: Reaction mixture for Actin qPCR

Reagents	Volume (μL)
5x Luna [®] Universal qPCR Master Mix	5
Actin Primer (Forward primer + Reverse Primer)	0.25
qH ₂ O	2.75
Template (1:10)	2
Total Volume	10

For the qPCR reaction, a Roche LightCycler[®] 96 was utilized to facilitate the temperature cycling required for amplification exponentially in real time and uses fluorescent dyes to monitor the amplification process. The qPCR reaction was carried out using a reaction volume of 10μL. After the qPCR amplification, the melt curve was analysed and the resulting products were electrophoresed on a 1.5% agarose gel.

Table 3.27: Thermal cycles for qPCR amplification

Cycle Step	Temperature (°C)	Time (s)	Cycles
Preincubation	95	300	1
Denaturation	95	15	35
Annealing	55	20	
Extension	72	10	
Melting	95	10	1
	65	60	
	97	1	
Cooling	37	30	1

3.2.11 PCR for E2 Knockout confirmation in mRNA level

To confirm the knockout of E2 domain in SIRT1 at the mRNA level, a PCR was done in cDNA synthesized from the isolated RNA samples. The PCR process involves multiple cycles of denaturation, annealing and extension to amplify the target cDNA sequence. Specific primers were designed to amplify SIRT1 full length and SIRT1-ΔE2 as mentioned in the **Table 3.13**. SIRT1 E1 internal forward primer with E5 Reverse primer amplifies SIRT1 full length and E1-E3 junction forward primer with E5 Reverse primer amplifies SIRT1-ΔE2. The PCR reaction

mixtures were prepared by combining the necessary reagents mentioned in **Table 3.28** and **Table 3.29**, and the PCR amplification was carried out using the conditions outlined in **Figure 3.4**.

Table 3.28: Reaction mixture of PCR for SIRT1 Full length

Reagents	Volume (μL)
2x Luna [®] Universal qPCR Master Mix	5
SIRT1 E1 Internal Forward Primer	0.5
E5 Reverse Primer	0.5
qH ₂ O	2
Template	2
Total Reaction Volume	10

Table 3.29: Reaction mixture of PCR for SIRT1-ΔE2

Reagents	Volume (μL)
2x Luna [®] Universal qPCR Master Mix	5
E1-E3 Junction Forward Primer	0.5
E5 Reverse Primer	0.5
qH ₂ O	2
Template	2
Total Reaction Volume	10

For the PCR reaction, an Eppendorf[®] Multiplex Thermocycler was utilized to facilitate the temperature cycling required for amplification. Prior to conducting the full reaction, a test was performed to determine the optimal annealing temperature. Various annealing temperatures were tested to identify the temperature at which the primers could efficiently bind to their complementary sequences in the cDNA template, ensuring successful amplification. Once the optimal annealing temperature was determined, the full PCR reaction was carried out using a reaction volume of 10μL. After the PCR amplification, the resulting products were electrophoresed on a 1.5% agarose gel.

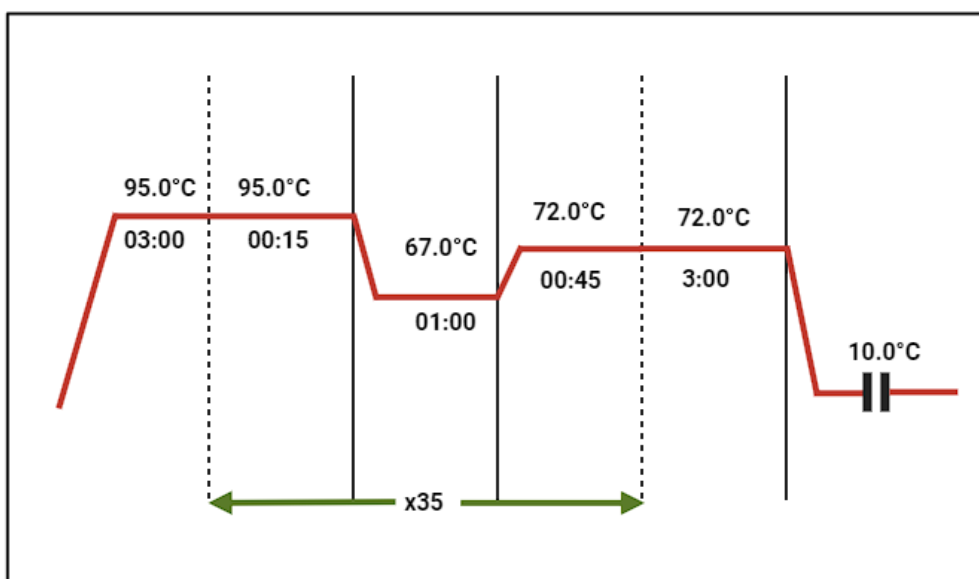


Figure 3.4: Schematic representation of PCR parameters employed during execution

3.2.11 Western blot for gene expression analysis in 24 months old mice liver samples

A preliminary work to provide valuable insights into the implication of exon 2 of SIRT1 in metabolic regulation during aging processes in protein level, we have done western blot analysis for key regulatory factors downstream SIRT1 signalling particularly in the context of aging in 24 months old mice liver samples in the condition of fed and starvation. The lysate preparation was done as mentioned in the section 3.2.4 and standard curve was generated to quantify the protein concentration in the samples as mentioned in the section 3.2.5. We have targeted SIRT1, PGC-1 α , AKT, pAKT, FOXO1, pFOXO1, CREB, pCREB and β -Tubulin for normalization and control. Western blot was employed as mentioned in the section 3.2.6 with the Primary antibodies specific to the targets mentioned in **Table 3.6** and 1:6000 ratio of Anti-Rabbit IgG-Peroxidase secondary antibody in 5% milk. Secondary antibody was used for SIRT1, PGC-1 α , AKT, FOXO1, CREB were used for the incubation. As the sizes of the proteins of AKT, pAKT and β -Tubulin lies between 63kDa to 48kDa, Stripping buffer was used to strip the analyzed AKT and pAKT. Then the blots were incubated with the Primary antibody specific to β -Tubulin and incubated with 1:6000 ratio of Anti-Mouse IgG-Peroxidase secondary antibody in 5% milk. After incubation the blots were washed in 1x TBST as mentioned in the section 3.2.6.4 and the targeted proteins were visualized as mentioned in the section 3.2.6.5. Then the images of the targeted proteins were quantified using ImageJ software.

3.2.12 Intraperitoneal Glucose Tolerance Test

In order to assess glucose homeostasis, an intraperitoneal glucose tolerance was performed on 3 months old six male C57/BL6 mice. This established in vivo approach investigates an organism's ability to regulate blood glucose levels following a glucose challenge. The day before the experiment, the mice were transferred to clean cages with no food with only access of drinking water. The animals were fasted for approximately 12 hours. On the day of the experiment, glucose solution was prepared with saline PBS about 2g/kg of bodyweight. The mice were marked in numerical order and their weights were noted to calculate the volume of Intra peritoneal glucose injection (μL) i.e., $10 \times \text{body weight (g)}$. To record the baseline fasting blood glucose level for each mouse, the tip of the tail of each mouse was carefully punctured using a needle and a small drop of blood was placed on the designated area of the strip which is inserted in the glucometer. Thus, the baseline fasting blood glucose level for each mouse was recorded. Then, the mice were administered respective dose of glucose solution intraperitoneally and the blood glucose levels were measured at 15, 30, 60 and 120 minutes following the glucose injection. For subsequent measurements, bleeding was reinitiated by removing the clot formed from their initial puncture. At the experiment's conclusion, food was provided in the cages for the mice, along with ensuring continued access to water. Then blood glucose levels over time were plotted to assess glucose tolerance.

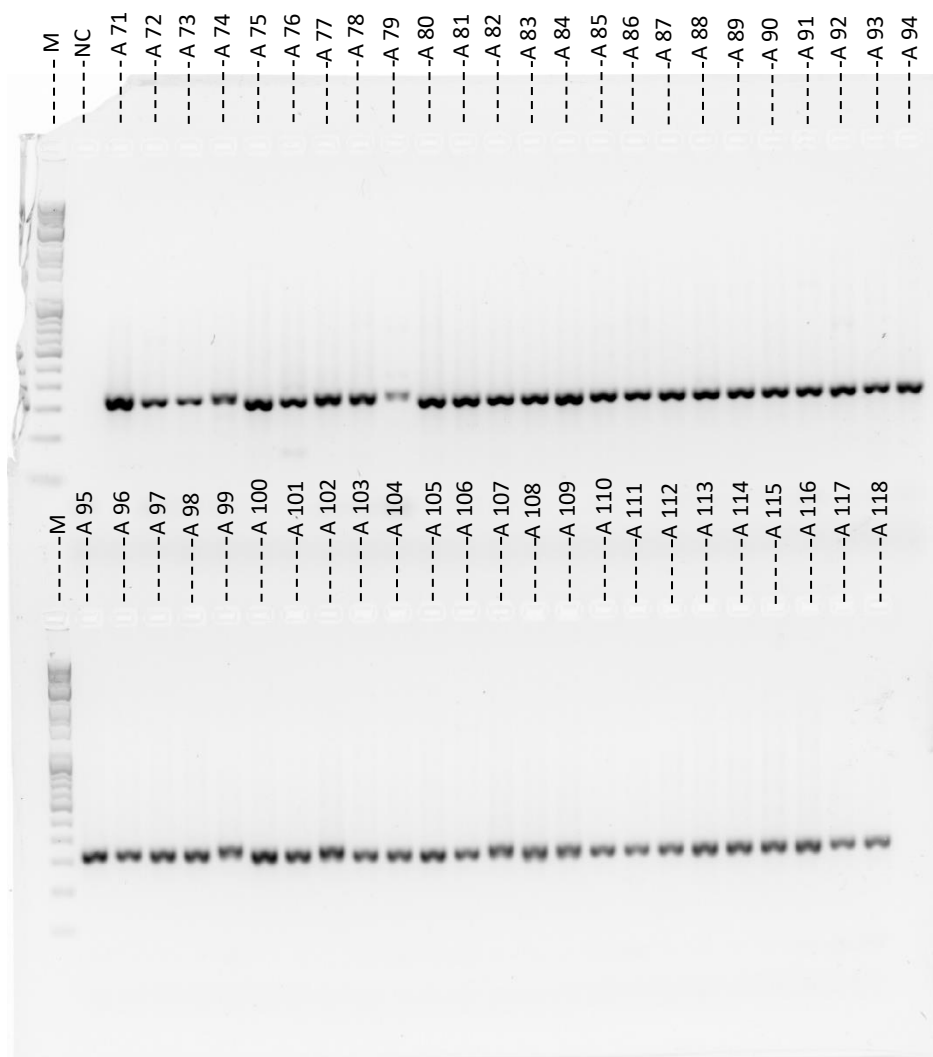
CHAPTER 4

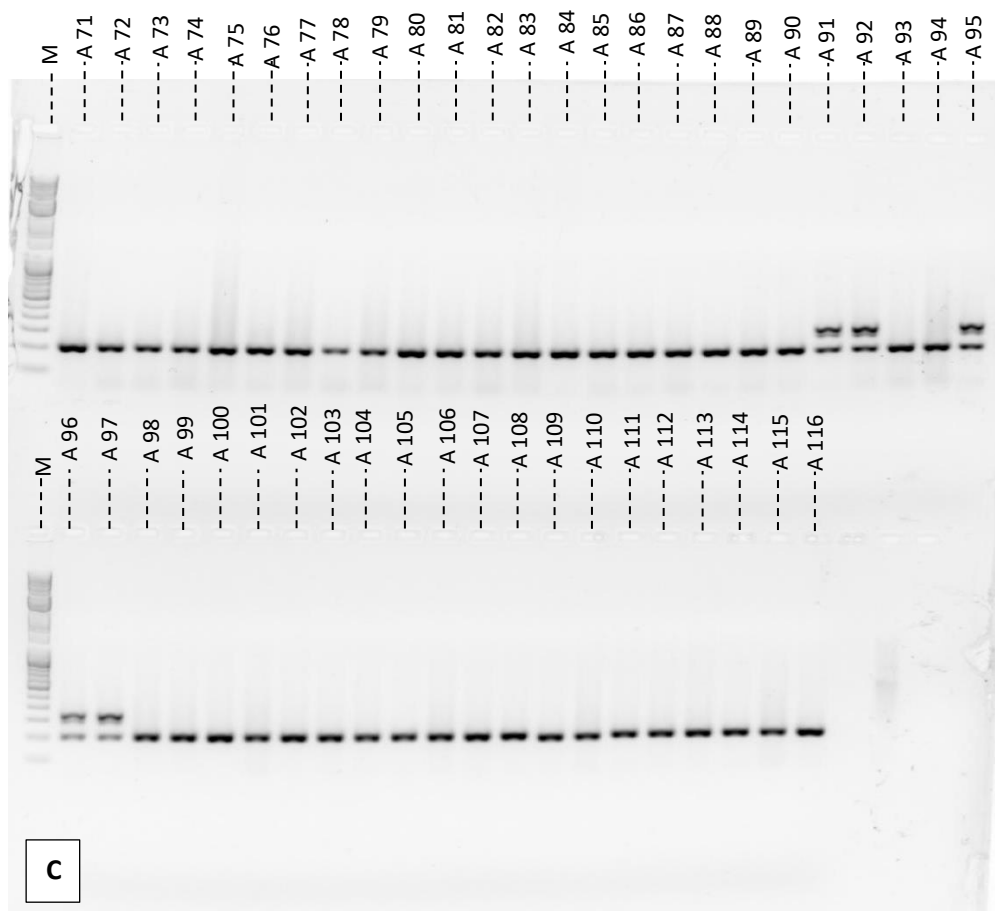
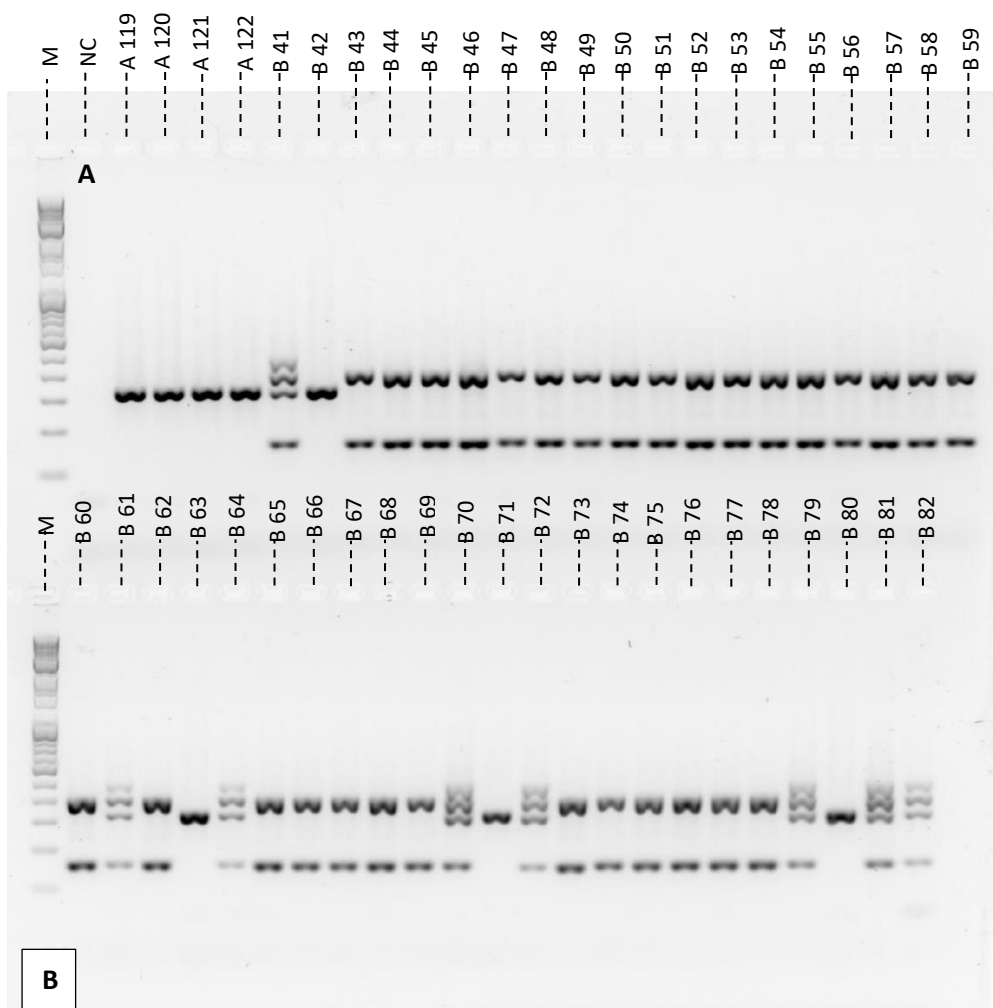
RESULTS

4. Results

4.1 Genotyping by PCR

Liver-specific SIRT1- Δ E2 mouse models (EC17IC) were generated by cre lox system following the protocol mentioned in the section 3.2.1 and those were grouped into wildtypes and knockouts. To make sure that they are the expected genotype, tail clips of all animals from both groups were collected to isolate genomic DNA by tail clip digestion following the protocol mentioned in the section 3.2.2 and subjected to genotyping by PCR guided by the specific primers designed to target the Albumin Cre sequences and LoxP sites (Table 3.11). The amplified genotyping PCR products were visualized by electrophoresis on 2% (w/v) agarose gel for Albumin Cre PCR products and 1.5% (w/v) agarose gel for LoxP PCR products and are displayed in **Figure 4.1 A-D**. Figure 4.1 A and B presents the agarose gel electrophoresis for the genotyping PCR amplifications of Albumin Cre, confirming all mice in wildtypes are homozygous and in knockouts 42, 63, 71 and 80 are homozygous, rest is heterozygous for the CRE loci. Figure 4.1 C and D presents the agarose gel electrophoresis for the genotyping PCR amplifications of LoxP sites, confirming 91, 92, 95, 96, 97, 118, 120 and 122 are heterozygous, rest is homozygous in wildtypes and all are homozygous in knockouts.





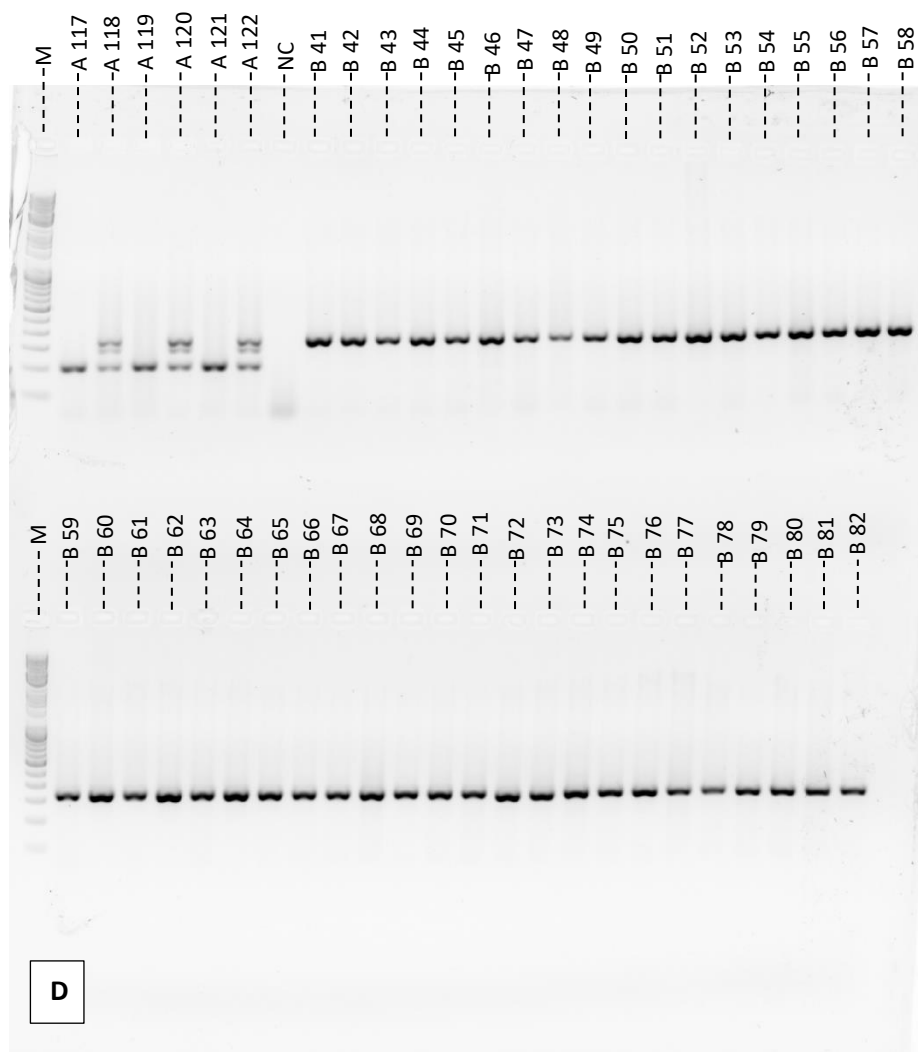


Figure 4.1: Genotyping and Visualization of (A and B) EC17IC A&B Albumin Cre and (C and D) EC17IC A&B E2lox/lox

A) Lane M-1 kb plus DNA marker, Lane 1-Negative control, Lane 2 to 49 - EC17IC A

B) Lane M-1 kb plus DNA marker, Lane 1-Negative control, Lane 2 to 5 - EC17IC A, Lane 6 to 49 - EC17IC B

C) Lane M-1 kb plus DNA marker, Lane 1to 46 – EC17IC A

D) Lane M-1 kb plus DNA marker, Lane 1 to 6 – EC17IC A, Lane 7 – Negative control, Lane 8 to 49- EC17IC B. Were, EC17IC A – Wildtype; EC17IC B - Knockout

4.2 Lysate preparation and BCA assay

Next, a mouse from wildtype and Knockout were sacked in the morning by Arushi S, a PhD student in the lab, liver and testes from each mouse were collected and dipped in liquid nitrogen to freeze them quickly and stored in -80°C . Then those tissues were lysed to prepare lysates by following the protocol mentioned in the section 3.2.4. To measure the total concentration of protein in those lysates, BCA assay was done by following the protocol mentioned in the section 3.2.5. A standard curve is prepared using a known protein, Bovine Serum Albumin (BSA), which is displayed in **Figure 4.2**. By comparing the samples absorbance to the standard curve, the protein concentration of samples lysates was determined.

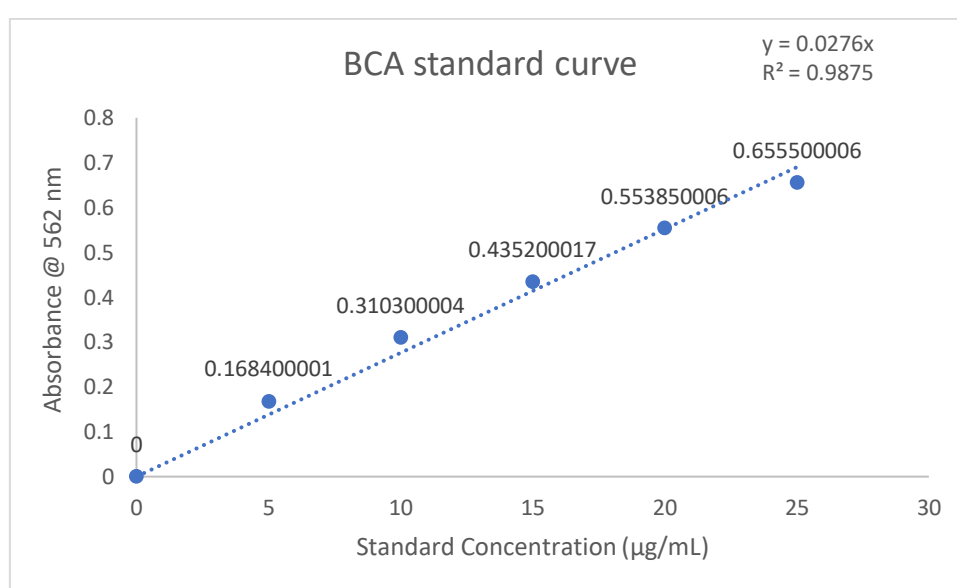


Figure 4.2: Standard curve for BCA Protein Assay of liver and testes

This standard curve was generated using duplicate measurements for each standard concentration and the R-squared value for the regression line is 0.9964.

4.3 Western Blot analysis to confirm SIRT1-ΔE2 Knockout

Western blot analysis with the standard concentration of $60\mu\text{g/mL}$ of proteins extracted from lysate preparation of wildtype and knockout liver samples and $30\mu\text{g/mL}$ of proteins extracted from lysate preparation of testes samples by following the protocol mentioned in the section 3.2.6 using the specific antibodies against SIRT1 and β -tubulin as a loading control (Table 3.6). Then, to detect the proteins in the membrane, chemiluminescence technique was performed according to the protocol mentioned in the section 3.2.6.5. As expected, **Figure 4.3** shows a band corresponding to the full-length SIRT1 was observed in the wildtype lanes. However, the size of this band was reduced in the knockout lanes, indicating the successful knockout of the ΔE2 domain of SIRT1. The bands were determined to be detect between 135 bp to 100 bp,

which corresponds to the expected sizes resulting from the western blot analysis confirming E2 domain knockout in SIRT1. Importantly, the β -tubulin band was present in all lanes with similar intensity in wildtype and knockout lanes determined between 63 bp to 48 bp, confirming equal protein loading across samples.

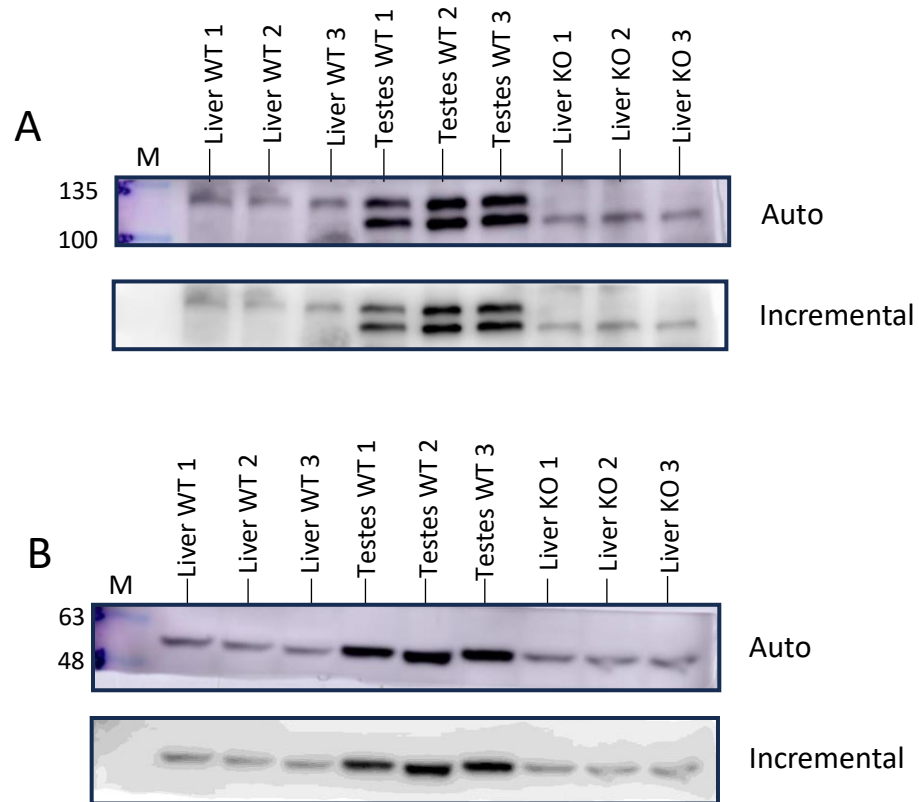


Figure 4.3: SIRT1- Δ E2 Knockout confirmation on western blots

A) SIRT1: Lane M – Protein marker, Lane 1 to 3 – EC17IC A, Lane 4 to 6 – EC17IC A, Lane 7 to 9 – EC17IC B

B) β -Tubulin: Lane M – Protein marker, Lane 1 to 3 – EC17IC A, Lane 4 to 6 – EC17IC A, Lane 7 to 9 – EC17IC B

4.4 Isolation of RNA

rRNA from the respective liver tissues of both wildtype and knockout samples were isolated by TRIzol method following the protocol mentioned in the section 3.2.7. The isolated rRNA was visualized by electrophoresis on 1.5% (w/v) agarose gel and is displayed in **Figure 4.4**. The rRNA is visible as distinct bands on the gel, it is used as an indicator of intact undegraded RNA thus confirming the successful isolation of RNA. The gel image also includes DNA size markers, which allow estimation of the rRNA's size. The result obtained from the gel electrophoresis demonstrated the successful isolation of RNA.

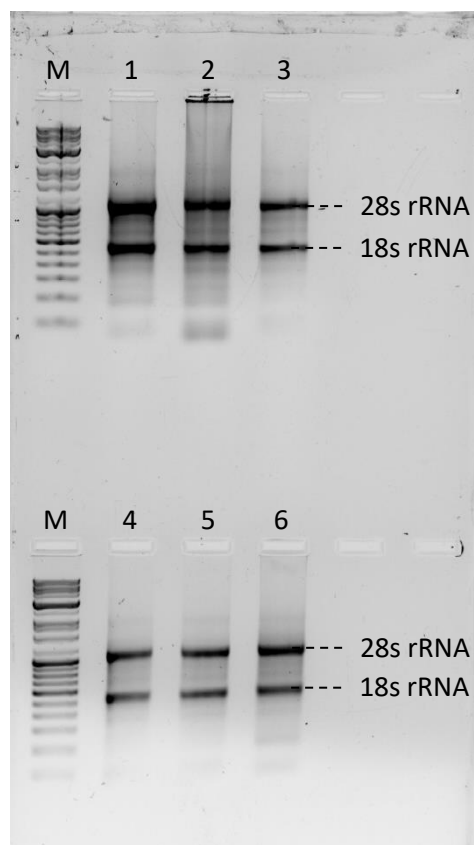


Figure 4.4: Isolation and visualization of RNA

Lane M – 1 kb plus DNA marker, Lane 1 to 3 – EC17IC A 1 to 3, Lane 4 to 6 – EC17IC B 1 to 3. Were, EC17IC A – Wildtype; EC17IC B - Knockout

4.5 Quantitative-PCR

Next, we went ahead to synthesize cDNA from the isolated RNA samples using SSIV RT kit from Invitrogen following the protocol mentioned in the section 3.2.8. Then, to ensure good quality of cDNA synthesis before proceeding with the downstream application to conform SIRT1- Δ E2 knockout, we performed qPCR for Actin following the protocol described in section 3.2.9, which can serve as a preliminary quality control step for my cDNA templates. The average Ct values for Actin across EC17IC A1, A2 and A3 are 19.01, 18.87 and 19.57 and for EC17IC B1, B2 and B3 are 18.93, 19.09 and 18.4 with the standard deviation of 0.3 in both EC17IC A and B. Melt curve for Actin across the samples were displayed in the **Figure 4.5 A**. The amplified qPCR products were visualized by electrophoresis on 1.5% (w/v) agarose gel. **Figure 4.5 B** displays consistent amplification of actin in cDNA across the samples, suggesting good cDNA quality for downstream applications.

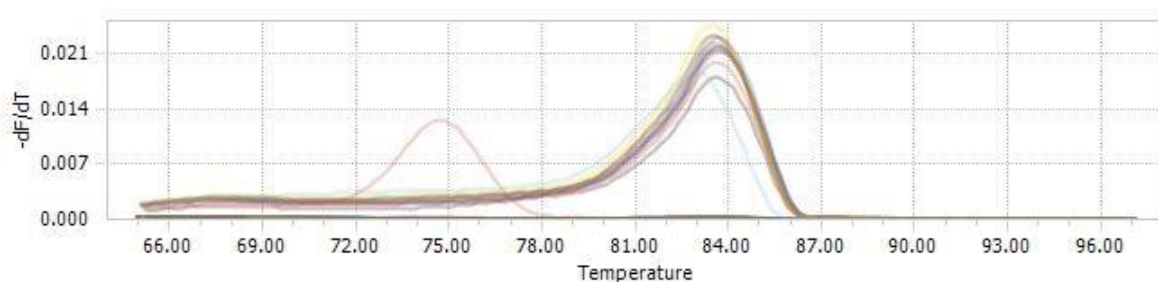


Figure 4.5 A: Melt curve for Actin in cDNA

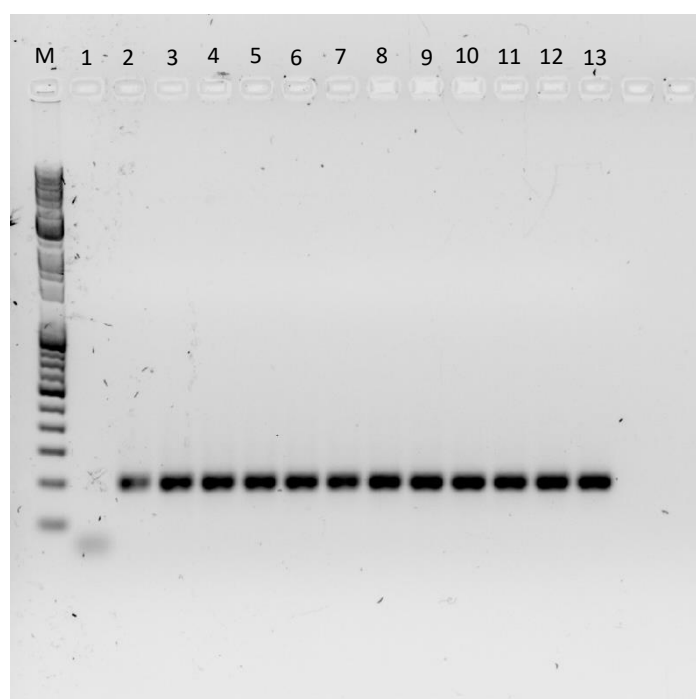


Figure 4.5 B: qPCR amplification of Actin in cDNA

Lane M – 1 kb plus DNA marker, Lane 1 – Negative control, Lane 2 & 3 – EC17IC A 1, Lane 4 & 5 – EC17IC A 2, Lane 6 & 7 – EC17IC A 3, Lane 8 & 9 – EC17IC B 1, Lane 10 & 11 – EC17IC B 2, Lane 12 & 13 – EC17IC B 3. Were, EC17IC A – Wildtype; EC17IC B - Knockout

4.6 Confirmation of SIRT1-ΔE2 knockout in cDNA

To confirm the SIRT1-ΔE2 knockout in mRNA level, we did PCR amplification of synthesized cDNA guided by the specific primers designed to target SIRT1 full length in wildtypes and SIRT1-ΔE2 in knockouts (Table 3.13) by following the protocol mentioned in the section 3.2.10. The amplified PCR products were visualized by electrophoresis on 1.5% (w/v) agarose gel and is displayed in **Figure 4.6**. The SIRT1 full length and SIRT1-ΔE2 amplification is visible as distinct bands on the gel, confirming the successful SIRT1-ΔE2 knockout. The gel

image also includes DNA size markers, which allow estimation of the SIRT1 full length and SIRT1- Δ E2 knockout. SIRT1 full length with SIRT1 E1 internal forward primer + E5 reverse primer bands size was determined to be 734 bp, and SIRT1- Δ E2 with SIRT1 E1 internal forward primer + E5 reverse primer bands size was determined to be 617 bp, and SIRT1- Δ E2 with E1-E3 junction + E5 reverse primer bands size was determined to be 561 bp, which corresponds to the expected bands sizes resulting from the PCR amplification of cDNA confirming E2 domain knockout in SIRT1.

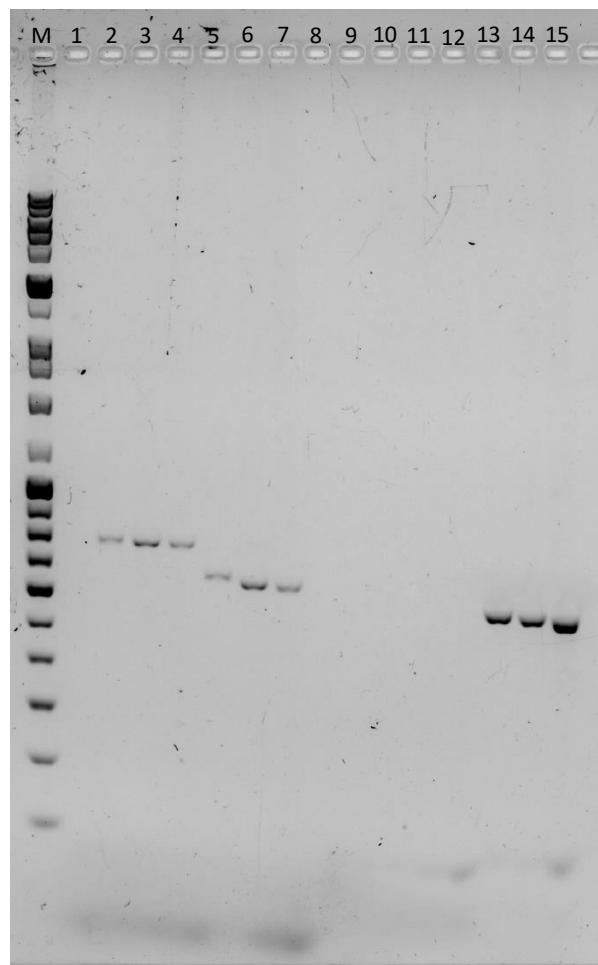


Figure 4.6: Confirmation of SIRT1- Δ E2 knockout in cDNA

Lane M – 1 kb plus DNA markers, Lane 1 – Negative control I, Lane 2 EC17IC A 1, Lane 3 – EC17IC A 2, Lane 4 – EC17IC A 3, Lane 5 – EC17IC B 1, Lane 6 – EC17IC B 2, Lane 7 - EC17IC B 3, Lane 8 – Empty well, Lane 9 – Negative control II, Lane 10 – EC17IC A 1, Lane 11 – EC17IC A 2, Lane 12-EC17IC A 3, Lane 13 – EC17IC B 1, Lane 14 – EC17IC B 2, Lane 15 – EC17IC B 3. Were, EC17IC A – Wildtype; EC17IC B - Knockout

4.7 Western Blot for Gene Expression Analysis in 24 months old mice liver samples

Western blot for gene expression analysis with the standard concentration of 30µg/mL of proteins extracted from the lysate preparation of SIRT1 full length (wildtype) and SIRT1-ΔE2 (knockout) liver samples of Ad libitum and 12 hours starved conditioned mice by following the protocol mentioned in the section 3.2.11 using the specific antibodies against SIRT1, PGC-1α, FOXO1, pFOXO1, AKT, pAKT, CREB, pCREB, and β-tubulin as a loading control (Table 3.6). Then to detect the proteins in the membrane, enhanced chemiluminescence technique was performed according to the protocol mentioned in the section 3.2.6.5. **Figure 4.7 A and B** displays gene expression quantification by ImageJ software for all proteins which are mentioned above, which shows that SIRT1 expression levels are slightly increased in the knockout of Ad libitum than the wild type but in 12 hours starvation there was not a change in the expression levels between the wildtype and knockout. Overall, SIRT1 were slightly reduced in 12 hours starvation when compared to the Ad libitum. PGC-1α expression levels is reduced in the knockout of Ad libitum compared to the wildtype but in 12 hours starvation, the expression level in knockout is slightly increased compared to the wildtype were increased in 12 hours starvation than the wildtype. Overall, PGC-1α were significantly increased in 12 hours starvation compared to the ad libitum. The expression level of pFOXO1/FOXO1 in knockout of ad libitum is slightly reduced when compared to the wildtype and also in 12 hours starvation, the expression is reduced in the knockout compared to the wildtype. But overall, the expression levels of pFOXO1/FOXO1 in 12 hours starvation was slightly increased when compared to the Ad libitum. The expression levels of pCREB/CREB are slightly increased in the knockout of Ad libitum but in 12 hours starvation, the expression level is slightly reduced in the knockout compared to the wildtype. Overall, the expression levels of pCREB/CREB are reduced in 12 hours starvation when compared to the Ad libitum. The expression level of pAKT/AKT in knockout of ad libitum is slightly reduced compared to the wildtype and also in 12 hours starvation, the expression level is reduced in the knockout compared to the wildtype. Overall, the expression levels of pAKT/AKT are slightly increased in the 12 hours starvation when compared to the Ad libitum. Fold change of AKT and CREB showed the levels in 12 hours starvation knockout is increased while FOXO1 levels in 12 hours starvation knockout is decreased.

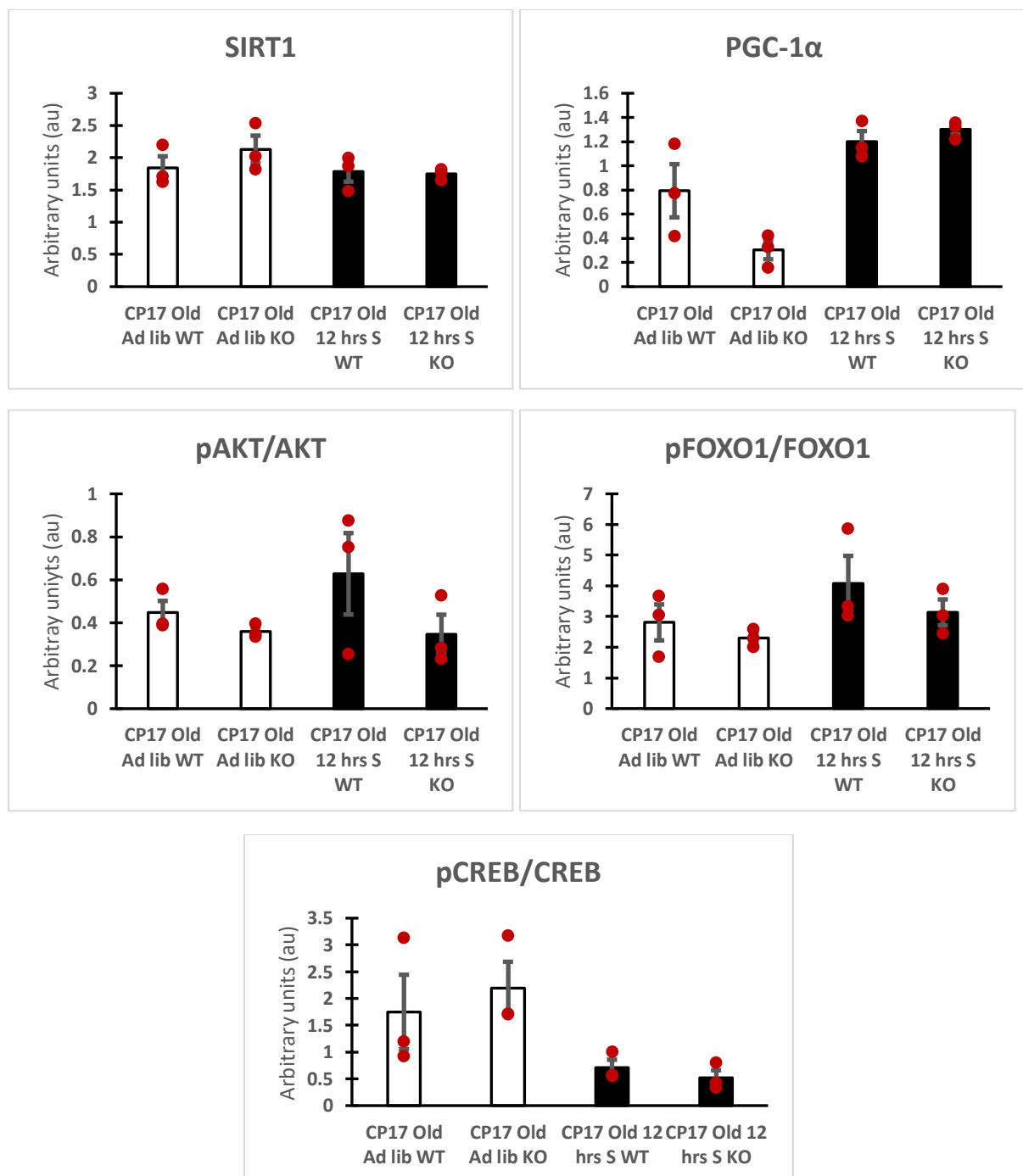


Figure 4.7 A: Quantified Protein Levels

Western blots were used to analyse genes involved in liver metabolism of 24 months old mice. SIRT1-CP17 Old Ad libitum wildtype (n=3) (SEM-0.17), CP17 Old Ad libitum liver Knockout (n=3) (SEM-0.2), CP17 12 hours starvation wildtype (n=3) (SEM-0.15), CP17 12 hours starvation liver knockout (n=3) (SEM-0.05). PGC-1 α -CP17 Old Ad libitum wildtype (n=3) (SEM-0.7), CP17 Old Ad libitum liver Knockout (n=3) (SEM-0.3), CP17 12 hours starvation wildtype (n=3) (SEM-1.2), CP17 12 hours starvation liver knockout (n=3) (SEM-1.3). pAKT/AKT-CP17 Old Ad libitum wildtype (n=3) (SEM-0.05), CP17 Old Ad libitum liver Knockout (n=3) (SEM-0.01), CP17 12 hours starvation wildtype (n=3)

(SEM-0.1), CP17 12 hours starvation liver knockout (n=3) (SEM-0.09). pCREB/CREB-CP17 Old Ad libitum wildtype (n=3) (SEM-0.7), CP17 Old Ad libitum liver Knockout (n=3) (SEM-0.5), CP17 12 hours starvation wildtype (n=3) (SEM-0.1), CP17 12 hours starvation liver knockout (n=3) (SEM-0.1). pFOXO1/FOXO1-CP17 Old Ad libitum wildtype (n=3) (SEM-0.5), CP17 Old Ad libitum liver Knockout (n=3) (SEM-0.1), CP17 12 hours starvation wildtype (n=3) (SEM-0.9), CP17 12 hours starvation liver knockout (n=3) (SEM-0.4).

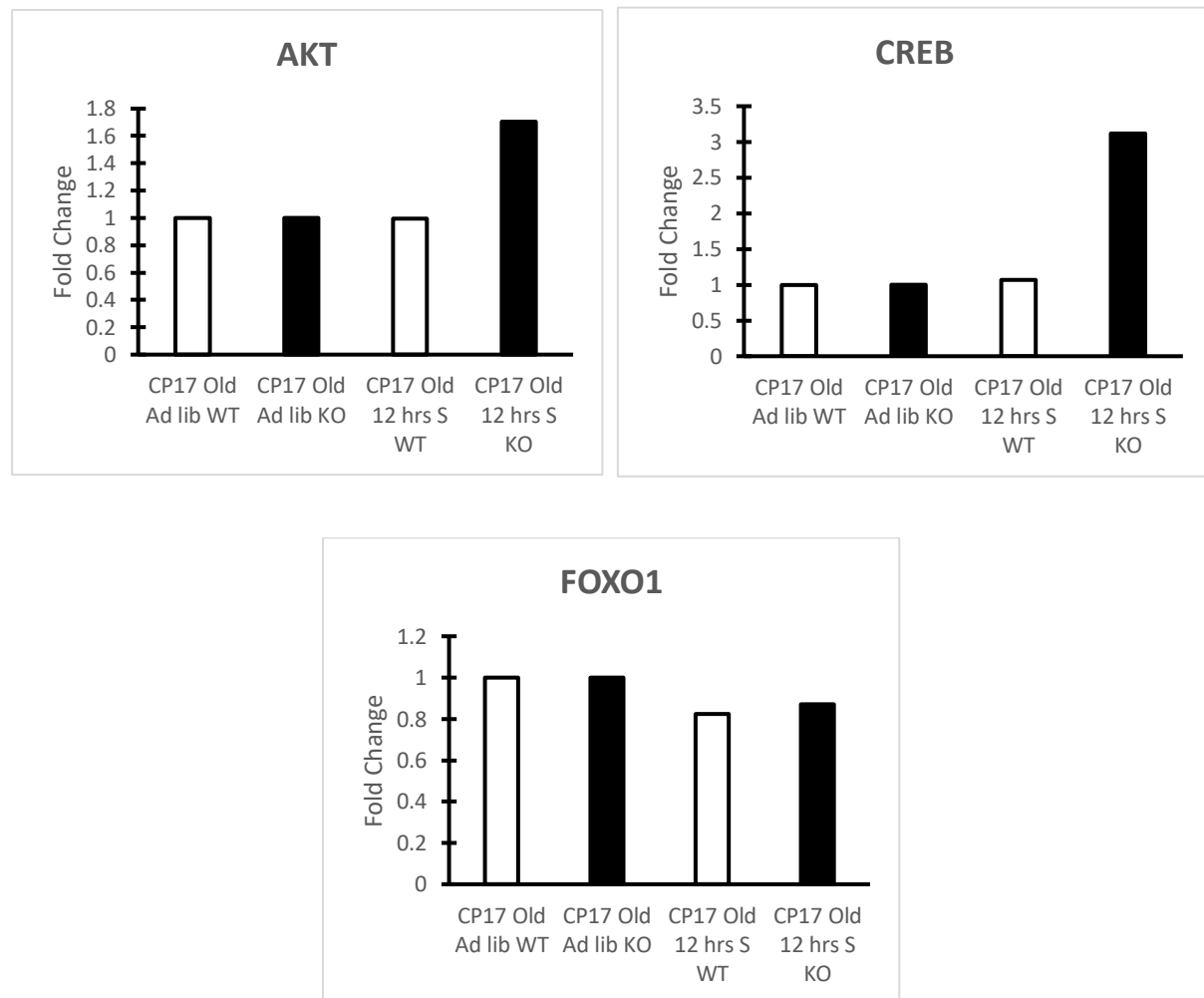


Figure 4.7 B: Fold change levels

AKT-CP17 Old Ad libitum wildtype (n=3), CP17 Old Ad libitum liver Knockout (n=3), CP17 12 hours starvation wildtype (n=3), CP17 12 hours starvation liver knockout (n=3). CREB-CP17 Old Ad libitum wildtype (n=3), CP17 Old Ad libitum liver Knockout (n=3), CP17 12 hours starvation wildtype (n=3), CP17 12 hours starvation liver knockout (n=3). FOXO1-CP17 Old Ad libitum wildtype (n=3), CP17 Old Ad libitum liver Knockout (n=3), CP17 12 hours starvation wildtype (n=3), CP17 12 hours starvation liver knockout (n=3).

4.8 Intraperitoneal Glucose Tolerance Test

Intraperitoneal Glucose Tolerance Test was performed on 3 months old, six male C57BL6/N mice by following the protocol mentioned in the section 3.2.12. The body weight, volume of IP glucose injection, baseline blood glucose level and blood glucose levels at different time intervals were mentioned in **Table 4.1**. The blood glucose levels over time were plotted to assess glucose tolerance by using GraphPad Prism software which is displayed in **Figure 4.8** in which the following parameters were analysed here: glucose concentration at basal level and at each time point after glucose administration and the dynamic of the curve decrease. The average of basal blood glucose level is 135mg/dL which is higher than the normal and after the glucose administration it peaks in 30 minutes and also after 120 minutes the blood glucose levels didn't reach the normal level.

Table 4.1: IP-GTT Data

Mouse		1	2	3	4	5	6
Body weight after 12 hours starvation (g)		30.3	27.8	28.8	30.2	30.3	38.5
Volume of IP injection (µL)		300	280	290	300	300	380
		Blood Glucose Levels (mg/dL)					
Time (minutes)	0	132	146	120	152	119	141
	15	259	289	200	391	250	321
	30	358	379	247	317	304	362
	60	334	279	235	282	286	300
	120	153	135	177	149	159	171

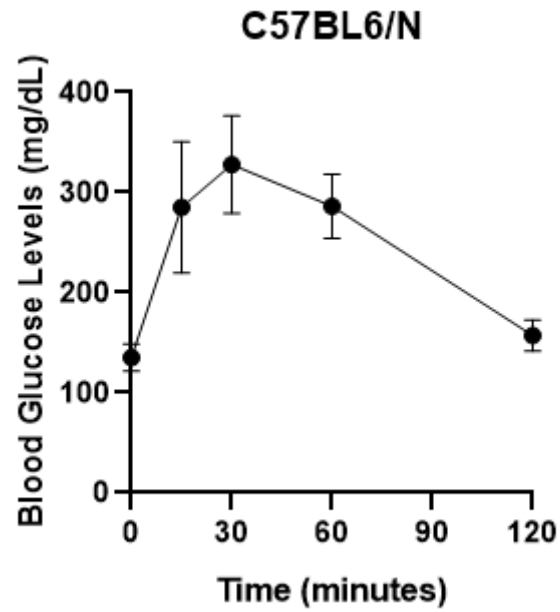


Figure 4.8: Blood glucose levels over time

GTT in 12 hours starvation of C57BL6/N, 3 months old male mice received IP injection of 20% glucose. The blood glucose levels (mg/dL) were measured at different time points using hand held glucometer.

CHAPTER 5

DISCUSSION

5. Discussion

SIRT1 is a key regulator of cellular metabolism with profound effects on hepatic physiology. To gain deeper insights into how the E2 domain influences SIRT1 signalling and liver metabolism particularly in the context of aging, we investigated the expression levels of key regulatory factors downstream of SIRT1 signalling in liver-specific SIRT1- Δ E2 knockout mice compared to wildtype mice.

In the first phase of our project, we have generated liver specific SIRT1- Δ E2 mouse models (EC17IC) by Cre-Lox system. Knockout techniques like Cre-lox allows for conditional gene knockouts, where the gene is inactivated only in cells expressing a specific Cre recombinase enzyme. So, the validation should be done to confirm that the presence of lox site and the knockout thereafter affects the intended domain within the gene and does not result in introduction of stop mutations or affecting the expression of the SIRT1 gene.

This is crucial because genes like SIRT1 have multiple functional domains, and knocking out the entire gene might have unintended consequences. In order to validate the successful knockout of E2 domain of SIRT1 specifically in liver, we have done protein and mRNA level experiments. In protein levels, the generated mouse. In both levels, we have confirmed the successful knockout of E2 domain in SIRT1 specifically in liver. This validation verifies that the knockout of E2 domain in SIRT1 is specific to the liver tissue.

In the second phase of our project, we focused on gene expression analysis of key regulatory factors downstream of SIRT1 signalling particularly in the context of aging. PGC-1 α for its well-established downstream target of SIRT1 and is known to regulate gluconeogenesis, fatty acid oxidation and mitochondrial biogenesis, which are crucial for efficient energy production in the liver. Understanding the PGC-1 α expression in KO mice would provide insights into how E2 domain deletion impacts substrate utilization in the liver, especially in aged mice where these processes are often compromised. FOXO1 is a transcription factor activated by SIRT1 deacetylation and plays a crucial role in gluconeogenesis, stress response and promoting longevity. Examining FOXO1 expression would help us determine if the E2 domain knockout affects SIRT1's ability to regulate gluconeogenesis and the cellular response to stress, potentially impacting metabolic health in aged mice. Another transcription factor involved in diverse cellular processes, including gluconeogenesis is CREB. Investigating CREB expression can help us understand the broader metabolic effects of E2 domain knockout. AKT is a central player in insulin signalling and a key regulator of various metabolic processes.

SIRT1 can deacetylate and activate AKT, influencing glucose uptake and metabolism. By analysing AKT and pAKT expression, we can explore potential changes in insulin sensitivity and nutrient signalling in the absence of E2 domain. By examining the expression profiles of these key targets, this study aims to decipher the specific contribution of the E2 domain to SIRT1 signalling and its impact on hepatic metabolic adaptation in aged mice under feeding and starvation conditions.

Our findings on SIRT1, PGC-1 α , FOXO1, CREB and AKT expression in old aged liver-specific SIRT1- Δ E2 knockout mice compared to wildtype mice reveal intriguing insights into the regulation of SIRT1 signalling and metabolic adaptation during feeding (ad libitum) conditions and starvation conditions.

Aging is known to be associated with decreased SIRT1 activity but we observed slight increase in SIRT1 protein levels in E2 domain knockout mice fed ad libitum compared to wildtype suggests a potential compensatory mechanism. Interestingly, during starvation, SIRT1 expression did not differ between genotypes. The overall reduction in SIRT1 expression in both WT and KO mice during starvation aligns with previous reports on decreased SIRT1 activity in aged animals. This downregulation might be a consequence of accumulated cellular stress and reduced NAD⁺ levels, a crucial SIRT1 cofactor, often observed in aging.

The reduced PGC-1 α expression in KO mice fed ad libitum suggests that the E2 domain is essential for optimal PGC-1 α protein levels. PGC-1 α is a key regulator of gluconeogenesis and fatty acid oxidation, and its reduction in KO mice might contribute to impaired metabolic efficiency during aging. During starvation, PGC-1 α expression increased in both genotypes, suggesting a conserved response to maintain energy production.

The slight decrease in the pAKT/AKT ratio in KO mice under both feeding and starvation conditions suggests a potential role for the E2 domain in AKT activation by SIRT1. AKT signalling plays a crucial role in insulin sensitivity and glucose metabolism.

Deacetylated FOXO1 by SIRT1 is known to translocate to the nucleus and promote gluconeogenesis. The increase in pFOXO1/FOXO1 ratio during starvation indicates, even though FOXO1 protein is being produced, a larger portion might be getting phosphorylated, keeping it inactive possibly to perturb gluconeogenesis. The fold change of FOXO1 in KO mice of 12 hrs starvation was reduced, thus E2 knockout reduces the levels of FOXO1 due to the increase in the levels of AKT which phosphorylates FOXO1 and translocate to cytoplasm and inactivate them.

The overall decrease in pCREB/CREB ratio during starvation suggests that it gets perturbed might contribute to impaired metabolic efficiency during aging and the fold change of CREB in KO mice of 12 hours starvation was higher, thus E2 knockout reduced the inhibition of CREB.

These findings highlight the complex interplay between SIRT1 signalling, metabolic regulation and the aging process. The observed changes in protein expression in E2 domain knockout mice suggest potential contributions to age related metabolic decline.

In order to assess glucose homeostasis, an intraperitoneal Glucose Tolerance Test was performed in 12 hours starvation of 3 months old, male C57BL6/N mice. This established in vivo approach involved administration of a glucose solution directly into the peritoneal cavity, followed by measurement of blood glucose levels at defined time points. Generally, a healthy mouse with normal glucose tolerance shows a characteristic rapid rise in blood glucose, reaching its peak 15 minutes after the glucose challenge. Subsequent glucose uptake, primarily conducted by muscle, fat and liver-tissue leads to a gradual decrease of the blood glucose concentration to the normal level after 120 minutes. In our findings, the blood glucose reached its peak 30 minutes after the glucose challenge and the blood glucose concentration has reached to the normal level after 120 minutes of administration. Increase in 30 minutes might hint that these mice are likely to be prediabetic, but more experiments need to be done to ascertain this.

5.1 Future perspectives

Investigate the mechanisms underlying the observed changes in gene expression. This could involve analysing post-translational modifications of SIRT1 targets to determine if the E2 domain knockout affects their activity status.

Analyse downstream targets of these pathways to assess functional consequences in KO mice. Measuring mitochondrial activity, substrate utilization rates, and metabolic enzyme expression would provide more comprehensive picture of how SIRT1 signalling and E2 domain knockout impact metabolic function in aged animals.

Compare metabolic parameters (e.g., blood glucose levels, insulin sensitivity) between WT and KO mice under feeding and starvation conditions. This would allow for more holistic understanding of the impact of E2 domain Knockout on whole-body metabolism in the context of aging.

CHAPTER 6

SUMMARY AND CONCLUSION

6. Summary & Conclusion

In the first phase of the project, we successfully generated liver-specific SIRT1-ΔE2 mouse models using Cre-lox system and confirmed the knockout by western blot analysis. We also isolated RNA from the liver tissues and synthesized cDNA from the isolated RNA and confirmed the knockout in mRNA level by PCR amplification of synthesized cDNA. In the second phase of the project, we did western blots for gene expression analysis in 24 months old mice liver samples under ad libitum fed and 12 hours starvation conditions. We analysed the expression of key metabolic regulators, SIRT1, PGC-1 α , FOXO1, CREB and AKT which revealed intriguing insights into the interplay between SIRT1 signalling and metabolic adaptation in the context of aging. This analysis showed that SIRT1 protein levels were slightly higher in knockout of ad lib compared to wildtype mice. However, both genotypes displayed a decrease in SIRT1 expression during starvation, suggesting a potential age-related decline in SIRT1 activity. E2 domain knockout resulted in reduced PGC-1 α protein levels under fed conditions, indicating a potential role for the E2 domain in maintaining optimal PGC-1 α levels. Both genotypes exhibited increased PGC-1 α expression during starvation, suggesting a conserved response to maintain energy production. The pCREB/CREB ratio was higher in knockout mice fed ad libitum, while both genotypes displayed a decrease during starvation. This finding suggests that the age-related perturbations altering its activity that require further investigation. The pAKT/AKT ratio was slightly lower in knockout mice under both fed and fasted conditions, suggesting a potential role for the E2 domain in SIRT1-mediated AKT activation. Additionally, we assessed glucose homeostasis after 12 hours starvation in 3 months old, male C57BL6/N mice (n=6), in which the prediabetic signs were seen as the injected glucose were not cleared within the timepoints.

In conclusion, this work helped in confirming generation of liver specific knockout. In addition, a preliminary work to provide valuable insights into the implication of exon 2 of SIRT1 in metabolic regulation during aging processes. The observed changes in protein expression in E2 domain knockout mice highlight potential contributions to age-related metabolic decline. And in vivo approach to assess glucose homeostasis after 12 hours starvation in C57BL6/N mice provided valuable insights. Overall, this study paves the way for future investigations into targeting the SIRT1-ΔE2 as a potential strategy for mitigating age-related metabolic dysfunction in both in vitro and in vivo approaches.

CHAPTER 7

REFERENCES

7. References

1. Rui, L. (2014). Energy metabolism in the liver. *Comprehensive physiology*, 4(1), 177.
2. Alamri, Z. Z. (2018) The role of liver in metabolism an updated review with physiological emphasis. *International journal of basic & clinical pharmacology*, 7(11), 2271-2276.
3. Alves-Bezerra, M , & Cohen D. E (2017). Triglyceride metabolism in the liver. *Comprehensive physiology*, 8(1), 1.
4. Raddatz, D., & Ramadori, G. (2007). Carbohydrate metabolism and the liver. actual aspects from physiology and disease. *Zeitschrift fur Gastroenterologie*, 45(01), 51-62.
5. Mitra, V., & Metcalf, J. (2009). Metabolic functions of the liver. *Anaesthesia & Intensive Care Medicine*, 10(7), 334-335.
6. Chaudry, R., & Varacallo, M. (2018). Biochemistry, glycolysis.
7. Nguyen, P. H. U. O. N. G. T. R. A. N .G., Leray, V., Diez, M., Serisier, S., Bloc'h, J. L., Siliart, B., & Dumon, H. (2008). Liver lipid metabolism. *Journal of animal physiology and animal nutrition*, 92(3), 272-283.
8. Bideyan, L., Nagari, R., & Tontonoz, P. (2021). Hepatic transcriptional responses to fasting and feeding. *Genes & development*. 35(9-10), 635-657.
9. Chiang, J. (2014). Liver physiology: Metabolism and detoxification. 1770-1782.
10. Li, X. (2013). SIRT1 and energy metabolism. *Acta Biochim Biophys Sin*, 45(1), 51-60.
11. Zhu, Y., Yan, Y., Gius, D. R., & Vassilopoulos, A. (2013). Metabolic regulation of Sirtuins upon fasting and implication for cancer. *Current opinion in oncology*, 25(6), 630-636.
12. Ye, X., Li, M., Hou, Y., Gao, T., Zhu, G., & Yang, Y. (2017). Sirtuins in glucose and lipid metabolism. *Oncotarget* 8(1), 1845.
13. Deota, S., Chattopadhyay, T., Ramachandran, D., Armstrong, e., Camacho, b., Maniyadath, B., Fulzele, A., Gonzalez-de-peredo, A., Denu, J. M. & Kolthur-Seetharam, U. (2017). Identification of a tissue restricted isoform of SIRT1 defines a regulatory domain that encode specificity. *Cell reports*, 18(13), 3069-3077.
14. Haigis, M. C, & Sinclair, D. A. (2010). Mammalian sirtuins: biological insights and disease relevance. *Annual Review of Pathology: Mechanism of Disease*, 5, 253-295.
15. Tanno, M., Sakamoto, J., Miura, T., Shimamoto, K., & Horio, Y. (2007). Nucleocytoplasmic shuttling of the NAD⁺-dependent histone deacetylase SIRT1. *Journal of Biological Chemistry*, 282(9), 6823-6832.
16. Houtkooper, R. H., Canto, C., Wanders, R. J., & Auwerx, J. (2010). The secret life of NAD⁺: an old metabolite controlling new metabolic signaling pathways. *Endocrine reviews*, 31(2), 194-223.

17. Bordone, L., & Guarente, L. (2005). Calorie restriction, SIRT1 and metabolism: understanding longevity. *Nature reviews Molecular cell biology*, 6(4), 298-305.
18. JT, R. (2005). Nutrient control of glucose homeostasis through a complex of PGC-1alpha and SIRT1. *Nature*, 434, 113-118.
19. Yoshino, J., Mills, K. F., Yoon, M. J., & Imai, S. I. (2011). Nicotinamide mononucleotide, a key NAD⁺ intermediate, treats the pathophysiology of diet-and age-induced diabetes in mice. *Cell metabolism*, 14(4), 528-536.
20. Skokowa, J., Lan, D., Thakur, B. K., Wang, F., Gupta, K., Cario, G., Brechlin, A. M., Schambach, A., Hinrichsen, L., Meyer, G. and Gaestel, M., & Welte, K. (2009). NAMPT is essential for the G-CSF-induced myeloid differentiation via a NAD⁺-sirtuin-1-dependent pathway. *Nature medicine*, 15(2), 151-158.
21. Van der veer, E., Ho, O'Nall, C., Barbosa, N., Scott, R., Cregan, S. P., & Pickering, J. G. (2007). Extension of human cell lifespan by nicotinamide phosphoribosyltransferase. *Journal of Biological Chemistry*, 282(15), 10841-10845.
22. Van den Berghe, G (1991). The role of the liver in metabolism homeostasis: implications for inborn errors of metabolism. *Journal of inherited metabolic disease*, 14(4), 407-420.
23. Liu, Yi., Dentin, R., Chen, D., Hedrick, S., Ravnskjaer, K., Schenk, S., Milne, J., Meyers, D. J., Cole, P., Iii, J. Y. and Olefsky, J., & Montminy, M. (2008). A fasting inducible switch modulates gluconeogenesis via activator/coactivator exchange. *Nature*, 456(7219), 269-273.
24. Rodgers, J. T., & Puigserver, P. (2007). Fasting-dependent glucose and lipid metabolic response through hepatic sirtuin 1. *Proceedings of the National Academy of Sciences*, 104(31), 12861-12866.
25. Purushothaman, A., Schug, T. T., Xu, Q., Surapureddi, S., Guo, X., & Li, X. (2009). Hepatocyte-specific deletion of SIRT1 alters fatty acid metabolism and results in hepatic steatosis and inflammation. *Cell metabolism*, 9(4), 327-338.
26. Wang, R. H., Li, C., & Deng, C. X. (2010). Liver steatosis and increased ChREBP expression in mice carrying a liver specific SIRT1 null mutation under a normal feeding condition. *International journal of biological sciences*, 6(7), 682.
27. Li, Y., Xu, S., Giles, A., Nakamura, K., Lee, J. W., Hou, X., Donmez, G., Li, J., Luo, Z., Wallsh, K & Guarente, L. (2011). Hepatic overexpression of SIRT1 in mice attenuates endoplasmic reticulum stress and insulin resistance in the liver. *The FASEB Journal*, 25(5), 1664.
28. Tontonoz, P., & Spiegelman, B. M. (2008). Fat and beyond the diverse biology of PPAR-gamma. *Annu. Rev. Biochem.*, 77, 289-312.β

29. Picard, F., Kurtev, M., Chung, N., Topark-Ngarm, A., Senawong, T., Machado de Oliveira, R., Leid, M., McBurney, M.W. & Guarente, L. (2004). Sirt1 promotes fat mobilization in white adipocytes by repressing PPAR-gamma. *Nature*, 429(6993), 771-776.
30. Chalkiadaki, A., & Guarente, L. (2012). High-fat diet triggers inflammation-induced cleavage of SIRT1 in adipose tissue to promote metabolic dysfunction. *Cell metabolism*, 16(2), 180-188.
31. Baur, J., Pearson, K. J., Price, N. L., Jamieson, H. A., Lerin, C., Kalra, A., Prabhu, V. V., Allard, J. S., Lopez-Lluch, G., Lewis, K., & Sinclair, D. A. (2006). Resveratrol improves health and survival of mice on a high-calorie diet. *Nature*, 444(7117), 337-342.
32. Moynihan, K. A., Grimm, A. A., Plueger, M. M., Bernal-Mizrachi, E., Ford, E., Cras-Meneur, C., Permutt, M. A., & Imai, S. I. (2005). Increased dosage of mammalian Sir2 in pancreatic β cells enhances glucose-stimulated insulin secretion in mice. *Cell metabolism*, 2(2), 105-117.
33. Bordone, L., Motta, M. C., Picard, F., Robinson, A., Jhaia, U. S., Apfeld, J., McDonagh, T., Lemieux, M., McBurney, M., Szilvasi, A., & Guarente, L. (2006). Sirt1 regulates insulin secretion by repressing UCP2 in pancreatic β cells. *PLoS biology*, 4(2), e31.
34. Horvath, T. L., Diano, S., & Tschop, M. (2004). Brain circuits regulating energy homeostasis. *The Neuroscientist*, 10(3), 235-246.
35. Morton, G. J., Cummings, D. E., Baskin, D. G., Barsh, G. S., & Schwartz, M. W. (2006). Central nervous system control of food intake and body weight. *Nature*, 443(7109), 289-295.
36. Cakir, I., Perello, M., Lansari, O., Messier, N. J., Vaslet, C. A., & Nillni, E. A. (2009). Hypothalamic Sirt1 regulates food intake in a rodent model system. *PloS one*, 4(12), e8322.
37. Ramadori, G., Fujikawa, T., Fukuda, M., Anderson, J., Morgan, D. A., Mostoslavsky, R., Stuart, R. C., Perello, M., Vianna, C. R., Nillni, E. A., & Coppari, R. (2010). SIRT1 deacetylase in POMC neurons is required for homeostasis defenses against diet-induced obesity. *Cell metabolism*, 12(1), 78-87.
38. Odegaard, J. I., Ricardo-Gonzalez, R. R., Goforth, M.H., Morel, C. R., Subramanian, V., Mukundan, L., Eagle, A. R., Vats, D., Brombacher, F., Ferrante, A. W., & Chawla, A. (2007). Macrophage-specific PPAR γ controls alternative activation and improves insulin resistance. *Nature*, 447(7148), 1116-1120.
39. Suganami, T., & Ogawa, Y. (2010). Adipose tissue macrophages: their role in adipose tissue modeling. *Journal of leukocyte biology*, 88(1), 33-39.

40. Pfluger, P. T., Herranz, D., Velasco-Miguel, S., Serrano, M., & Tschop, M. H. (2008). Sirt1 protects against high-fat diet-induced metabolic damage. *Proceedings of the national academy of sciences*, 105(28), 9793-9798.
41. Yeung, F., Hoberg, J. E., Ramsey, C. S., Keller, M. D., Jones, D. R., Frye, R. A., & Mayo, M. W. (2004). Modulation of NF- κ B- dependent transcription and cell survival by the Sirt1 deacetylase. *The EMBO journal*, 23(12), 2369-2380.
42. Wijnen, H., & Young, M. W. (2006). Interplay of circadian clocks and metabolic rhythms. *Annu. Rev. Genet.*, 40, 409-448.
43. Wijnen, H. (2009). A circadian loop as SIRT's itself. *Science*, 324(5927), 598-599.
44. Turek, F. W., Joshu, C., Kohsaka, A., Lin, E., Ivanova, G., McDearmon, E., Laposky, A., Losee-Olson, S., Easton, A., Jensen, D. R., & Bass, J. (2005). Obesity and metabolic syndrome in circadian Clock mutant mice. *Science*, 308(5724), 1043-1045.
45. Kohsaka, A., Laposky, A. D., Ramsey, K. M., Estrada, C., Joshu, C., Kobayashi, Y., Turek, F. W., & Bass, J. (2007). High-fat diet disrupts behavioral and molecular circadian rhythms in mice. *Cell metabolism*, 6(5), 414-421.
46. Asher, G., Gatfield, D., Stratmann, M., Reinke, H., Dibner, C., Kreppel, F., Mostoslavsky, R., Alt, F. W. & Schibler, U. (2008). SIRT1 regulates circadian clock gene expression through PER2 deacetylation. *Cell* 134(2), 317-328.
47. Nakahata, Y., Sahar, S., Astarita, G., Kaluzova, M., & Sassone-Corsi, P. (2009). Circadian control of the NAD⁺ salvage pathway by CLOCK-SIRT1. *Science*, 324(5927), 654-657.
48. Trefts, E., Gannon, M., Wasserman, d. H. (2017). The liver. *Curbiol* 27:R1147-R1151.
49. Sutherland, E. W., & Cori, C. F. (1951). Effect of hyperglycemic-glycogenolytic factor and epinephrine on liver phosphorylase. *Journal of Biological Chemistry*, 188(2), 531-543.
50. Berg, J., Tymoczko, J. L., & Stryer, L., (2002). The regulation of cellular respiration is governed primarily by the need for ATP. *Biochemistry*, 5th ed.; WH Freeman: New York, NY, USA.
51. Alves-Bezerra, M., & Cohen, D. E. (2017). Triglyceride metabolism in the liver.. *Comprehensive physiology*, 8(1), 1.
52. Bideyan, L., Nagar, R., & Tontonoz, P. (2021). Hepatic transcriptional responses to fasting and feeding. *Genes & development*, 35(9-10), 635-657.
53. Kersten, S., Seydoux, J., Peters, J. M., Gonzalez, F. J., Desvergne, B., & Wahli, W (1999). Peroxisome proliferator-activated receptor α mediates the adaptive response to fasting. *The Journal of Clinical investigation*, 103(11), 1489-1498.

54. Cheon, Y., Nara, T. Y., Band, M. R., Beever, J. E., Wallig, M. A., & Nakamura, M. T. (2005). Induction of overlapping genes by fasting and a peroxisome proliferator in pigs: evidence of functional PPAR α in nonproliferating species. *American Journal of Physiology-Regulatory, Integrative and Comparative Physiology*, 288(6), R1525-R1535.
55. Potthoff, M. J., Inagaki, T., Satapati, S., Ding, X., He, T., Goetz, R., Mohammadi, M., Finck, B.N., Mangelsdorf, D.J., Kliewer, S. A., & Burgess, S. C. (2009). FGF21 induces PGC-1 α and regulates carbohydrate and fatty acid metabolism during the adaptive starvation response. *Proceedings of the National Academy of Sciences*, 106(26), 10853-10858.
56. Rhee, J., Inoue, Y., Yoon, J. C., Pigserver, P., Fan, M., Gonzalez, F. J., & Spiegelman, B. M. (2003). Regulation of hepatic fasting response by PPAR γ coactivator-1 α (PGC-1): requirement for hepatocyte nuclear factor 4 α in gluconeogenesis. *Proceedings of the national academy of sciences*, 100(7), 4012-4017.
57. Keller, H., Dreyer, C., Medin, J., Mahfouddi, A., Ozato, K., & Wahli, W. (1993). Fatty acids and retinoids control lipid metabolism through activation of peroxisome proliferator-activated receptor-retinoid X receptor heterodimers. *Proceedings of the National Academy of Sciences*, 90(6), 2160-2164.
58. Sanderson, L. M., Boekschoten, M. V., Desvergne, B., Müller, M., & Kersten, S. (2010). Transcriptional profiling reveals divergent roles of PPAR β/δ in regulation of gene expression in mouse liver. *Physiological genomics*, 41(1), 42-52.
59. Chakravarthy, M. V., Pan, Z., Zh, Y., Tordjman, K., Schneider, J. G., Coleman, t., Trk, J., & Semenkovich, C. F. (2005). "New" hepatic fat activates PPAR α to maintain glucose, lipid and cholesterol homeostasis. *Cell metabolism*, 1(5), 309-322.
60. Goldstein, I., Baek, S., Presman, D. M., Paakinaho, V., Swinstead, E. E., & Hager, G. L. (2017). Transcription factor assisted loading and enhancer dynamics dictate the hepatic fasting response. *Genome Research*, 27(3), 427-439.
61. Guan, G., Dai, P. H., Osborne, T. F., Kim, J.B., & Shecter, I. (1997). Multiple sequences elements are involved in the transcriptional regulation of the human squalene synthase gene. *Journal of Biological Chemistry*, 272(15), 10295-10302.
62. Shimano, H., Yahagi, N., Amemiya-Kudo, M., Hasty, A. H., Osuga, J. I., Tamura, Y., Shionoiri, F., Iizuka, Y., Ohashi, K., Harada, K., & Yamada, N. (1999). Sterol regulatory element-binding protein-1 as a key transcription factor for nutritional induction of lipogenic enzyme genes. *Journal of Biological Chemistry*, 274(50), 35832-35839.

63. Horton, J. D., Bashmakov, Y., Shimomura, I., & Shimano, H. (1998). Regulation of sterol regulatory element binding proteins in livers of fasted and refed mice. *Proceedings of the National Academy of Sciences*, 95(11), 5987-5992.
64. Lu, M., & Shyy, J. Y. J. (2006). Sterol regulatory element binding protein 1 is negatively modulated by PKA phosphorylation. *American Journal of physiology-cell physiology*, 290(6), C1477-C1486.
65. Ponungoti, B., Kim, D. H., Xiao, Z., Smith, z., Miao, J., Zang, M., Wu, S. Y., Chiang, C. M., Veenstra, T. D., & Kemper, J. K. (2010). SIRT1 deacetylates and inhibits SREBP-1C activity in regulation of hepatic lipid metabolism. *Journal of Biological Chemistry*, 285(44), 33959-33970.
66. Tong, X., Li, P., Zhang, D., VanDommelen, K., Gupta, N., Rui, L., Omary, M.B., & Yin, L. (2016). E4BP4 is an inulin-induced stabilizer of nuclear SREBP-1c and promotes SREBP-1c mediated lipogenesis[S]. *Journal of Lipid research*, 57(7), 1219-1230.
67. Janowski, B. A., Grogan, M. J., Jones, S. A., Wisely, G. B., Kliewer, S. A., Corey, E. J., & Mangelsdorf, D. J. (1999). Structural requirements of ligands for the oxysterol liver X receptors LXR α and LXR β . *Proceedings of the National Academy of Sciences*, 96(1), 266-271.
68. Anthonisen, E. H., Berven, L., Holm, S., Nygaard, M., Nebb, H. I., & Grønning-WANG, L. M. (2010). Nuclear receptor liver X receptor is O-GlcNAc-modified in response to glucose. *Journal of biological chemistry*, 285(3), 1607-1615.
69. Adamson, A. W., Suchankova, G., Rufo, C., Naakamura, M. T., Teran-Garcia, M., Clarke, S. D., & Gettys, T. W. (2006). Hepatocyte nuclear factor-4 α contributes to carbohydrate-induced transcriptional activation of hepatic fatty acid synthase. *Biochemical Journal*, 399(2), 285-295.
70. Fan, Q., Nørgaard, R. C., Bindesbøll, C., Lucas, C., Dalen, K. T., Babaie, E., Itkonen, H. M., Matthews, J., Nebb, H.I., & Grønning-Wang, L. M. (2017). LXR α regulates hepatic ChREBP α activity and lipogenesis upon glucose, but not fructose feeding in mice. *Nutrients*, 9(7), 678.
71. Kabashima, T., Kawaguchi, T., Wadzinski, B. E., & Uyeda, K. (2003). Xylulose 5-phosphate mediates glucose-induced lipogenesis by xylulose 5-phosphate-activated protein phosphatase in rat liver. *Proceedings of the National Academy of Sciences*, 100(9), 5107-5112.

72. Tao, R., Xiong, X., DePinho, R. A., Deng, c.X., & Dong, X. C. (2003). Hepatic SREBP-2 and cholesterol biosynthesis are regulated by FoxO3 and Sirt6[S]. *Journal of lipid research*, 54(10), 2745-2753.
73. Pfaffenbach, K. T., Nivala, A. M., Reese, L., Ellis, F., Wang, D., Wei, Y., & Pagliassotti, M. J. (2010). Rapamycin inhibits postprandial-mediated X-box-binding protein-1 splicing in rat liver. *The Journal of nutrition*, 140(5), 879-884.
74. Quinn, P. G., & Granner, D. K. (1990). Cyclic AMP-dependent protein kinase regulates transcription of the phosphoenolpyruvate carboxykinase gene but not binding of nuclear factors to the cyclic AMP regulatory element. *Molecular and cellular biology*, 3357-3364.
75. Lee, M. W., Chanda, D., Yang, J., Oh, H., Kim, S. S., Yoon, Y. S., Park, k. G., Lee, I. K., Choi, C. S., & Koo, S. H. (2010). Regulation of hepatic gluconeogenesis by an ER-bound transcription factor, CREBH. *Cell metabolism*, 11(4), 331-339.
76. Altarejos, J. Y., & Montminy, M. (2011). CREB and the CRTC co-activators: sensors for hormonal and metabolic signals. *Nature reviews Molecular cell biology*, 12(3), 141-151.
77. Koo, S. H., Flenchner, L., Qi, L., Zhang, X., Sreter, R. A., Jeffries, S., Hedrick, S., Xu, W., Boussouar, F., Brindle, P., & Takemori, H. (2005). The CREB coactivator TORC2 is a key regulator of fasting glucose metabolism. *Nature*, 437(7062), 1109-1114.
78. Dentin, R., Liu, Y., Koo, S. H., Hedrick, S., Vargas, T., Heredia, J., Yates III, J. & Montminy, M. (2007). Insulin modulates gluconeogenesis by inhibition of the coactivator TORC2. *Nature*, 449(160), 366-369.
79. Wang, Y., Vera, L., Fischer, W. H., & Montminy, M. (2009). The CREB coactivator CRTC2 links hepatic ER stress and fasting gluconeogenesis. *Nature*, 460(7254), 534-537.
80. Wu, Z., Jiao, P., Huang, X., Feng, B., Feng, Y., Yang, S., Hwang, P., Du, J., Nie, Y., Xiao, G., & Xu, H. (2010). MAPK phosphatase-3 promotes hepatic gluconeogenesis through dephosphorylation of forkhead box O1 in mice. *The Journal of clinical investigation*, 120(11), 3901-3911.
81. Nakae, J., Park, B. C., & Accili, D. (1999). Insulin stimulates phosphorylation of the forkhead transcription factor FKHR on serine 253 through a Wortmannin-sensitive pathway. *Journal of Biological Chemistry*, 274(23), 15982-15985.
82. Yoon, J. C., Puigserver, P., Chen, G., Donovan, J., Wu, Z., Rhee, J., Adelman, G., Stafford, J., Kahn, nC. R., Granner, D. K., & Newgard, C. B. (2001). Control of hepatic gluconeogenesis through the transcriptional coactivator PGC-1. *Nature*, 413(6852), 131-138.

83. Li, X., Monks, B., Ge, Q., & Bimbaum, M. J. (2007). Akt/PKB regulates hepatic metabolism by directly inhibiting PGC-1 α transcription coactivator. *Nature*, 447(7147), 1012-1016.
84. Rodgers, J. T., Lerin, C., Haas, W., Gygi, S. P., Spiegelman, B. M., & Puigserver, P. (2005). Nutrient control of glucose homeostasis through a complex of PGC-1 α and SIRT1. *Nature*, 434(7029), 113-118.
85. Lee, J. M., Seo, W. Y., Han, H. S., Oh, K. J., Lee, Y. S., Kim, D. K., Choi, S., Choi, B. H., Harris, R. A., Lee, C. H., & Koo, S. H. (2016). Insulin-inducible SMILE inhibits hepatic gluconeogenesis. *Diabetes*, 65(1), 62-73.
86. Opherk, C., Tronche, F., Kellendonk, C., Kohlmüller, D., Schulze, A., Schmid, W., & Schutz, G. (2004). Inactivation of the glucocorticoid receptor in hepatocytes leads to fasting hypoglycemia and ameliorates hyperglycemia in streptozotocin-induced diabetes mellitus. *Molecular endocrinology*, 18(6), 1346-1353.
87. Oh, K. J., Park, J., Kim, S. S., Oh, H., Choi, C. S., & Koo, S. H. (2012). TCF7L2 modulates glucose homeostasis by regulating CREB- and Fox O1 -dependent transcriptional pathway in the liver. *PLoS Genet*, 8.
88. Cassuto, H., Kochhan, K., Chakravarty, K., Cohen, H., Blum, B., Olswang, Y., Hakimi, P., XU, C., Massillon, D., Hanson, R. W., & Reshef, L. (2005). Glucocorticoids regulate transcription of the gene for phosphoenolpyruvate carboxykinase in the liver via an extended glucocorticoids regulatory unit. *Journal of Biological Chemistry*, 280(40), 33873-33884.
89. Ploton, M., Mazuy, C., Gheeraert, C., Dubois, V., Berthier, A., Dubois-Chevalier, J., Marechal, X., Bantubunji, K., Diemer, H., Cianferani, S., & Strub, J. M. (2018). The nuclear bile acid receptor FXR is a PKA- and FOXA2-sensitive activator of fasting hepatic gluconeogenesis. *Journal of hepatology*, 69(5), 1099-1109.
90. Kersten, S. (2014). Integrated physiology and systems biology of PPAR α . *Molecular metabolism*, 3(4), 354-371.
91. Rufo, C., Teran-Garcia, M., Nakamura, M. T., Koo, S. H., Towle, H. C., & Clarke, S. D. (2001). Involvement of a unique carbohydrate-responsive factor in the glucose regulation of rat liver fatty-acid synthase gene transcription. *Journal of Biological Chemistry*, 276(24), 21969-21975.
92. Iizuka, K., Bruick, R. K., Liang, G., Horton, J. D., & Uyeda, K. (2004). Deficiency of carbohydrate response element-binding protein (ChREBP) reduces lipogenesis as well as glycolysis. *Proceedings of the National Academy of Sciences*, 101(19), 7281-7286.

93. Stanya, K. J., Jacobi, D., Liu, S., Bhargava, P., Dai, L., Gangl, M. R., Inouye, K., Barlow, J. L., Ji, Y., Mizgerd, J. P., & Qi, L. (2012). Direct control of hepatic glucose production by interleukin-13 in mice. *The Journal of clinical investigation*, 123(1).
94. Nie, Y., Erion, D. M., Yuan, Z., Dietrich, M., Shulman, G. I., Horvath, T. L., & Gao, Q. (2009). STAT3 inhibition of gluconeogenesis is downregulated by SirT1. *Nature cell biology*, 11(4), 492-500.
95. Ramakrishnan, S. K., Zhang, H., Takahashi, S., Centofanti, B., Periyasamy, S., Weisz, K., Chen, Z., Uhler, M. D., Rui, L., Gonzalez, F. J., & Shah, Y. M. (2016). HIF2 α is an essential molecular brake for postprandial hepatic glucagon response independent of insulin signaling. *Cell metabolism*, 23(3), 505-516.
96. Oosterveer, M. H., Matak, C., Yamamoto, H., Harach, T., Moullan, N., Van Dijk, T. H., Ayuso, E., Bosch, F., Postic, C., Groen, A. K., & Auwerx, J. (2012). LRH-1-dependent glucose sensing determines intermediary metabolism in liver. *The Journal of clinical investigation*, 122(8), 2817-2826.
97. Liu, Y., Dentin, R., Chen, D., Hedrick, S., Ravnskjaer, K., Schenk, S., Milne, J., Meyers, D. J., Cole, P., Lii, J. Y., & Olefsky, J. (2008). A fasting inducible switch modulates gluconeogenesis via activator/coactivator exchange. *Nature*, 456(7219), 269-273.
98. Wang, F., & Tong, Q. (2009). SIRT2 suppresses adipocyte differentiation by deacetylating FOXO1 and enhancing FOXO1's repressive interaction with PPAR γ . *Molecular biology of the cell*, 20(3), 801-808.
99. Houtkooper, R. H., Pirinen, E., & Auwerx, J. (2012). Sirtuins as regulators of metabolism and healthspan. *Nature reviews Molecular cell biology*, 13(4), 225-238.
100. Hallows, W. C., Yu, W., & Denu, J. M. (2012). Regulation of Glycolytic Enzyme Phosphoglycerate Mutase-1 by Sirt1 protein-mediated Deacetylation. *Journal of Biological Chemistry*, 287(6), 3850-3858.
101. Zhou, S., Tang, X., & Chen, H. Z. (2018). Sirtuins and insulin resistance. *Frontiers in Endocrinology*, 9, 421838.
102. Hou, X., Xu, S., Maitland-Toolan, K., Jiang, B., Ido, Y., Lan, F., Walsh, K., Wierzbicki, M., Verbeuren, T. J., & Cohen, R. A. (2008). SIRT1 regulates hepatocyte lipid metabolism through activating AMP-activated protein kinase. *Journal of Biological Chemistry*, 283(29), 20015-20026.
103. Li, X., Zhang, S., Blander, G., Jeanette, G. T., Krieger, M., & Guarente, L. (2007). SIRT1 deacetylates and positively regulates the nuclear receptor LXR. *Molecular cell*, 28(1), 91-106.

104. Purushotham, A., Xu, Q., Lu, J. F., Yan, X., Kim, D. H., Kemper, J. K., & Li, X. (2012). Hepatic deletion of SIRT1 decreases hepatocyte nuclear factor 1 α /farnesoid X receptor signaling and induces formation of cholesterol gallstones in mice. *Molecular and cellular biology*, 32(7), 1226-1236.
105. Yang, X., Downes, M., Ruth, T. Y., Bookout, A. L., He, W., Straume, M., Mangelsdorf, D. J., & Evans, R. M. (2006). Nuclear receptor expression links the circadian clock to metabolism. *Cell*, 126(4), 801-810.
106. Hashimoto, T., Cook, W. S., Qi, C., Yeldandi, A. V., Reddy, J. K., & Rao, M. S. (2000). Defect in peroxisome proliferator-activated receptor α -inducible fatty acid oxidation determines the severity of hepatic steatosis in response to fasting. *Journal of biological chemistry*, 275(37), 28918-28928.
107. Herzig, S., Long, F., Jhala, U. S., Hedrick, S., Quinn, R., Bauer, A., Rudolph, D., Schutz, G., Yoon, C., Puigserver, P. & Spiegelman, B. (2001). CREB regulates hepatic gluconeogenesis through the coactivator PGC-1. *Nature*, 413(6852), 179-183.

CHAPTER 8
APPENDIX

8. Appendix

8.1 Preparation of Agarose gel

Horizontal agarose gel electrophoresis was carried out to visualize genotyping PCR products, qPCR products, PCR products and RNA samples. Varying gel percentage were used to separate the fragments of different sizes. The gels were prepared in 1X TAE buffer. The samples were electrophoresed at 120V and visualized using a UV transilluminator.

8.2 RNA concentration measurement

The NanoDrop™ One/One^C Microvolume UV-Vis Spectrophotometer was utilized to measure the RNA concentration, offering the advantage of not requiring sample dilution before measurement. The instrument was prepared for use by loading a water sample onto the lower measurement pedestal. To perform a sample measurement, a blank sample with 1 µL volume and the same solvent as the sample was loaded onto the lower measurement pedestal. The sampling arm was closed, and the “Blank” button was clicked to record the blank measurement. The pedestals were then wiped using a laboratory wipe. After the initial blank measurement, a 1 µL sample was pipetted onto the lower pedestal, and the sampling arm was closed again. The “Measure” button was clicked to initiate the measurement process. Once the measurement was completed, the sampling arm was opened, and the sample was carefully wiped from both the upper and lower pedestals using a laboratory wipe. This process of loading the sample, measuring, and wiping the pedestals was repeated for each sample.